Institut Matériaux Microélectronique Nanosciences de Provence

Compétition de grains et formation des défauts cristallins pendant la croissance du silicium par des méthodes *in situ* de diffraction X et microscopie électronique (EBSD)

Nathalie Mangelinck-Noël, nathalie.mangelinck@im2np.fr

H. Ouaddah, T. Riberi-Béridot, M. Tsoutsouva, M. Becker, G. Regula, G. Reinhart, I. Périchaud

L. Barrallier, F. Guittonneau

J. Baruchel, T.-N. Tran, E. Boller, M. Majkut, A. Rack, J.-P. Valade

Photovoltaic Si-cell fabrication chain

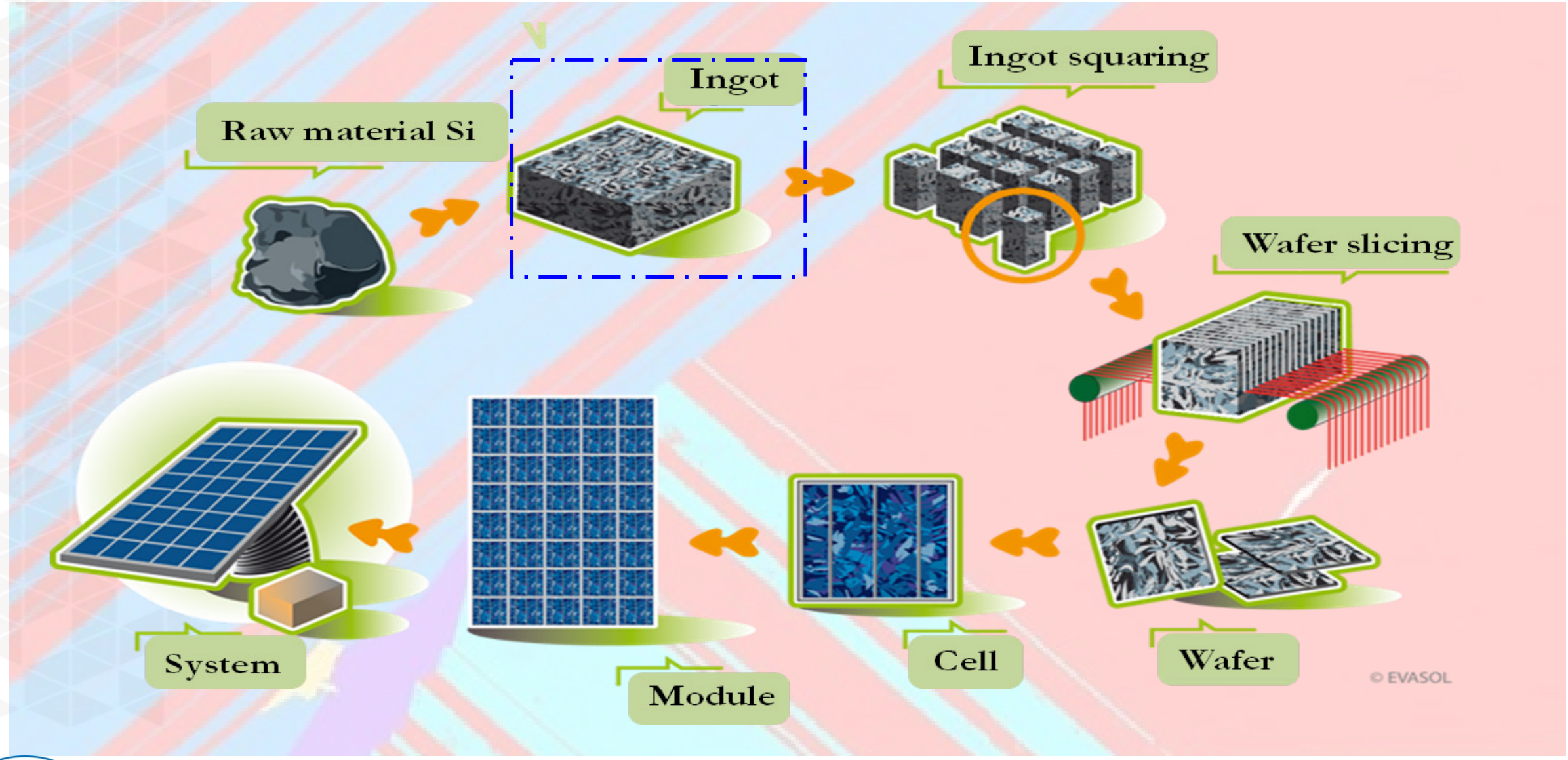

Photovoltaic Si-cell fabrication chain

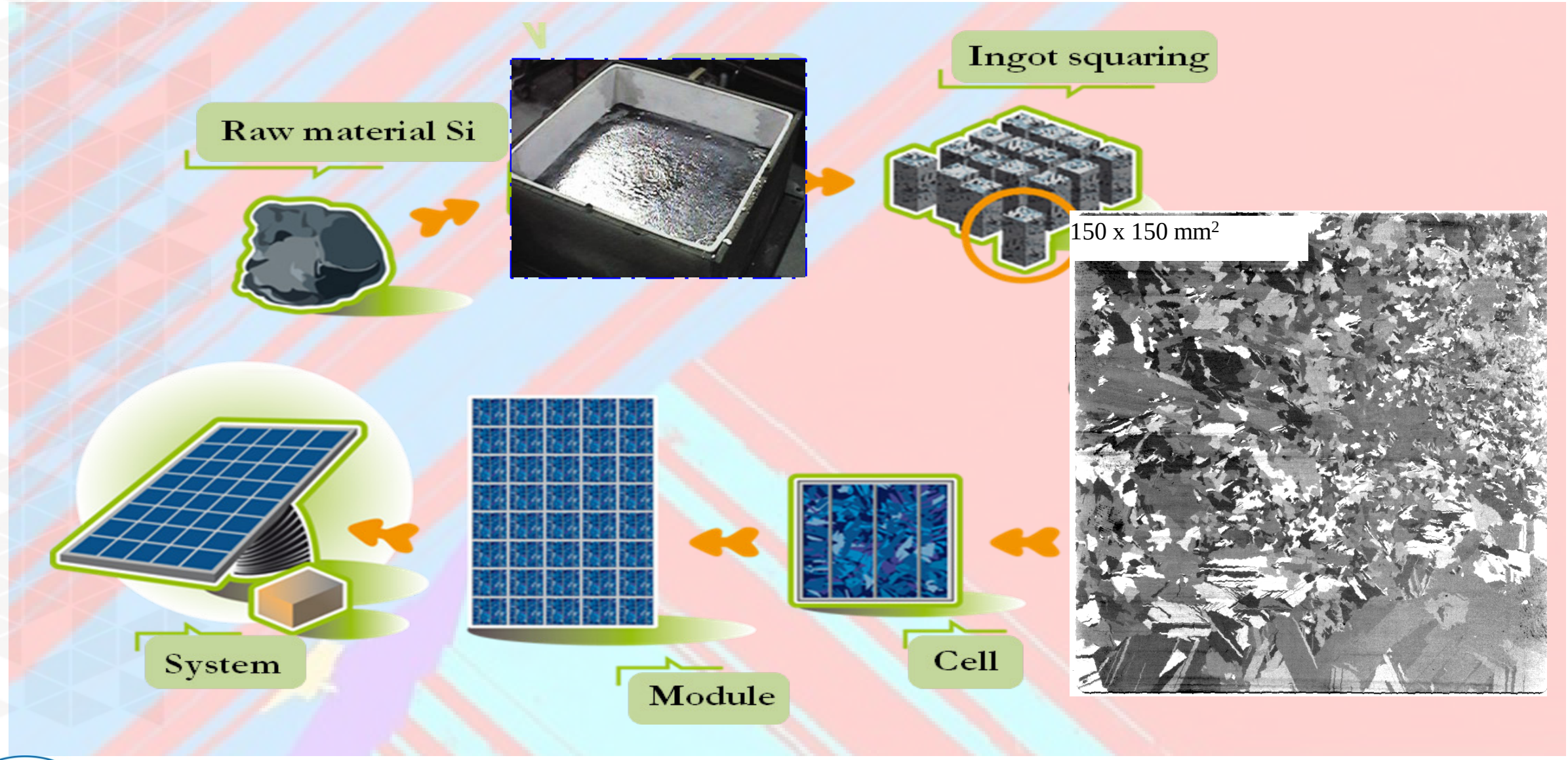

Solidification features / PV performance

The structural defects can be electrically active :

- **Grains** and **grain boundaries**
- **Twins** and **associated twin boundaries**

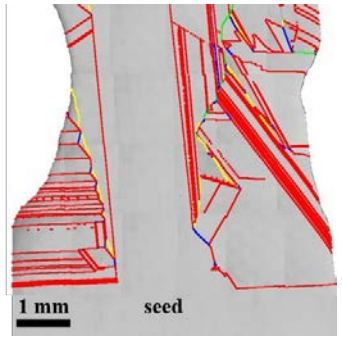

Σ3 <111>
Σ9 <110>
Σ27a <110>

M. Tsoutsouva et al. Acta Materialia 115 (2016) 210

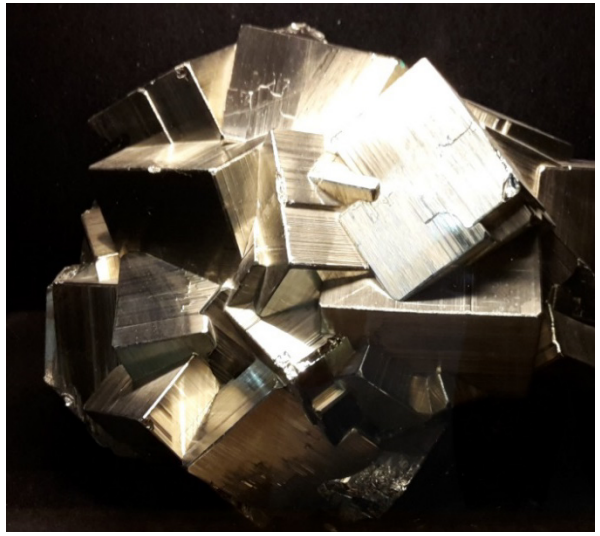

Peruvian Pyrite twins

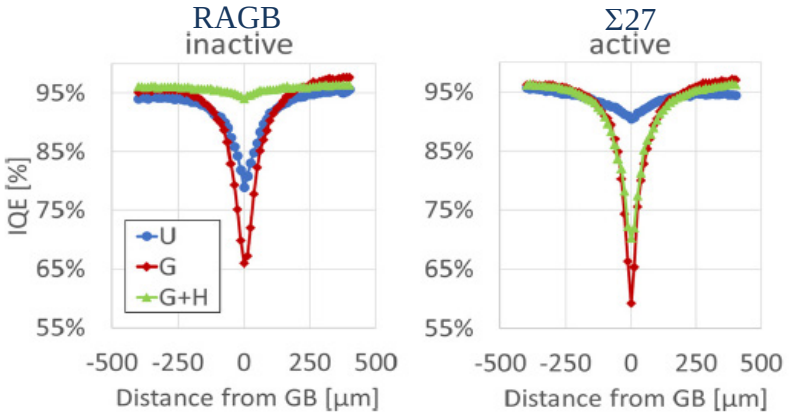

K. Adamczyk et al. JAP 123 (2018) 055705

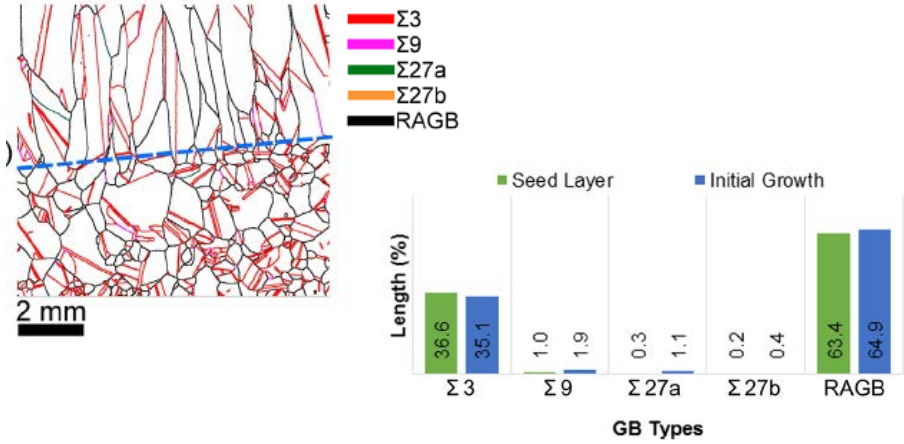

G.W. Alam et al. PSSC (2017) 1700177

Solidification features / PV performance

The structural defects can be electrically active and interact with impurities:

- **Grains** and **grain boundaries**
- **Twins** and **associated twin boundaries**
- **Sub-grain boundaries**
- **Dislocations**

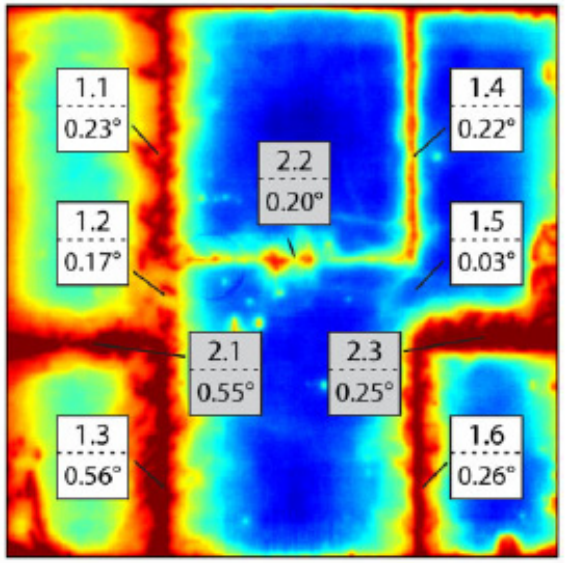

Trempa et al., J. Crystal Growth 312 (2010) 1517-15

Ekstrom et al. PSSA 212 N 10 (2015) 2278-2288

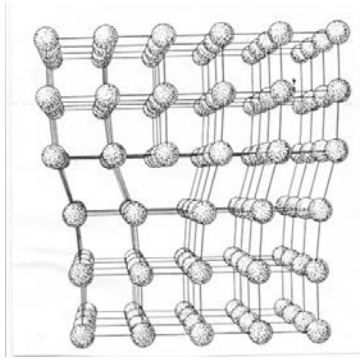

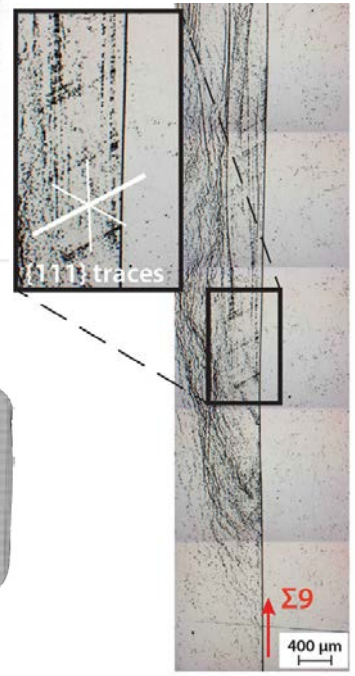

Autruffe et al. J. Cryst. Growth 411 (2015) 12-18

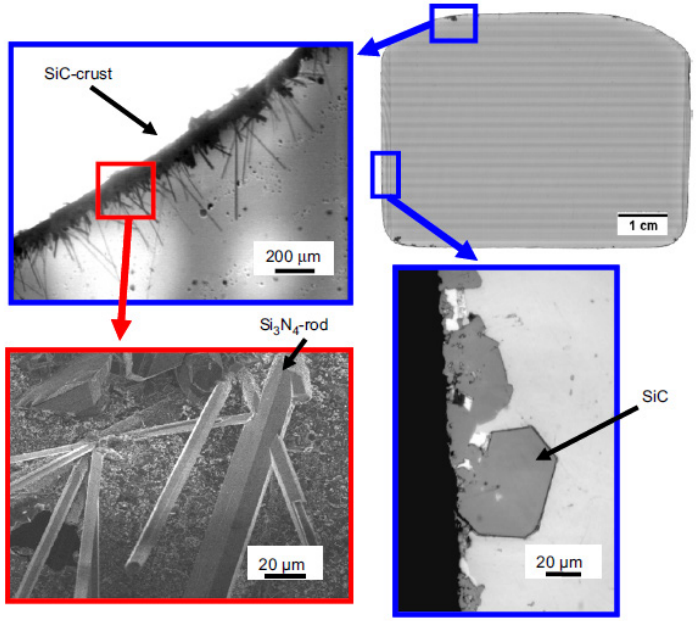

Originality of our work

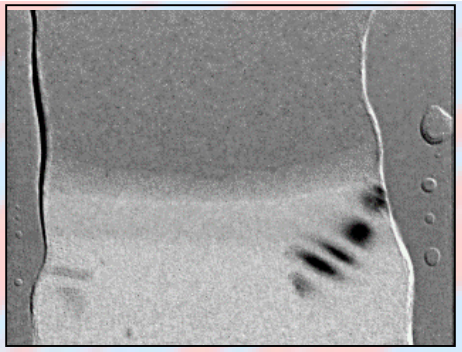
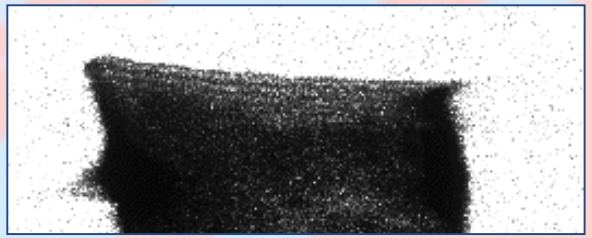


- **Investigate growth mechanisms** experimentally.
- ***In situ*** and **real-time X-ray imaging** during **solidification.**
- **Radiography** and **Topography (Bragg Diffraction Imaging).**
- **High temperature (up to 1800 °C).**


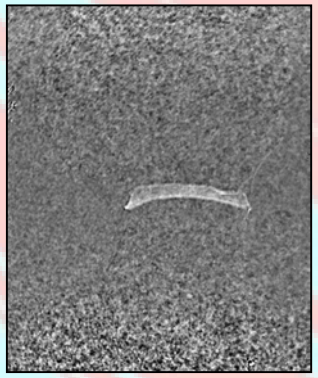


X-ray radiography

1895, Wilhelm Conrad Röntgen

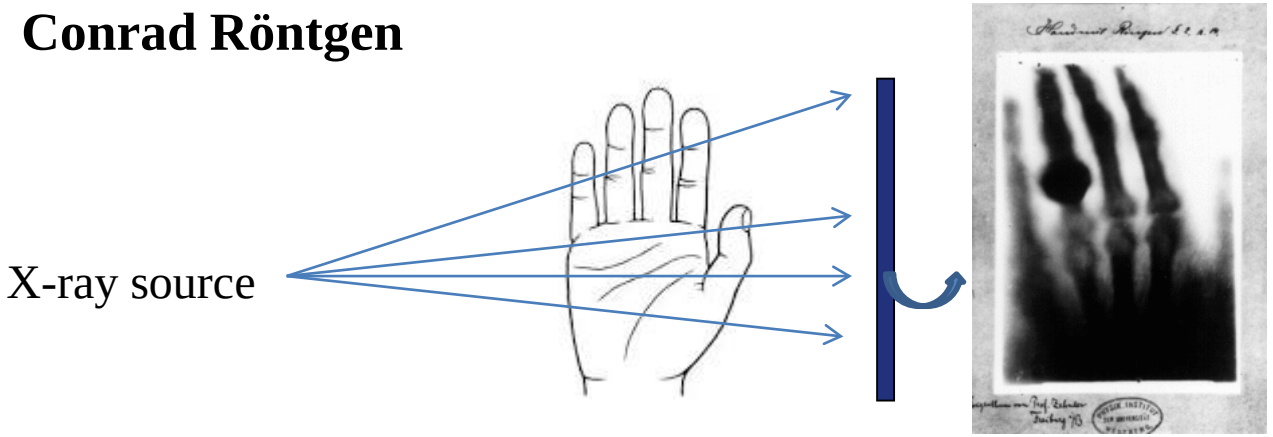

First X-ray radiography: hand of Anna Bertha Ludwig Röntgen December 22nd 1895

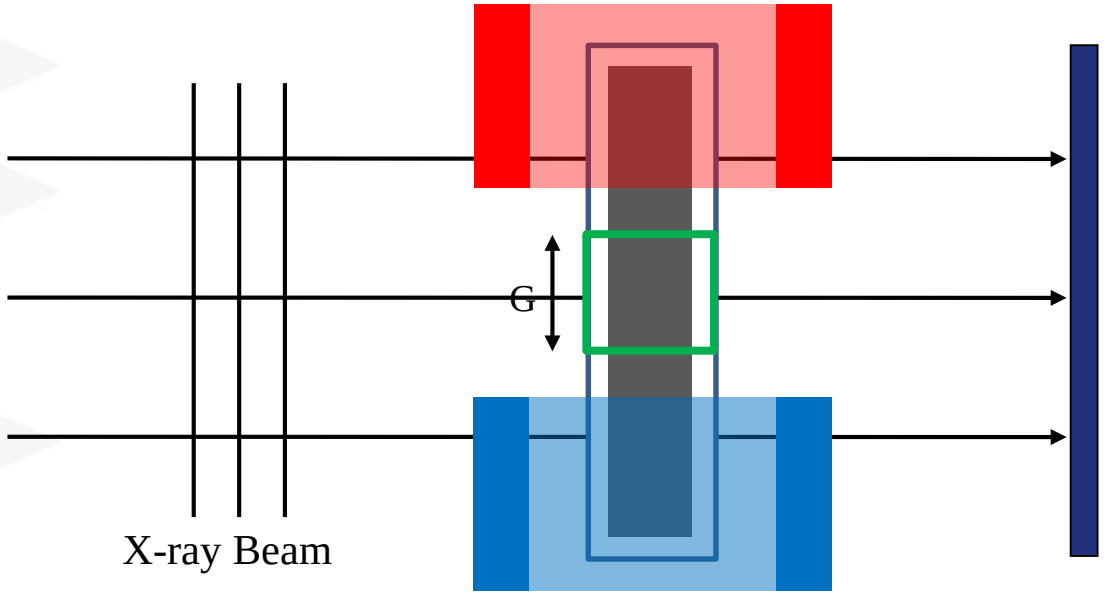

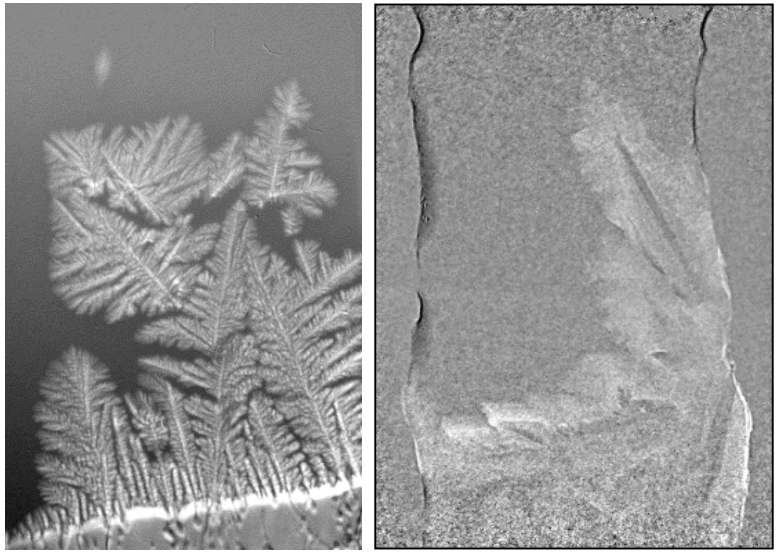

Images on camera

2 mm

X-ray radiography

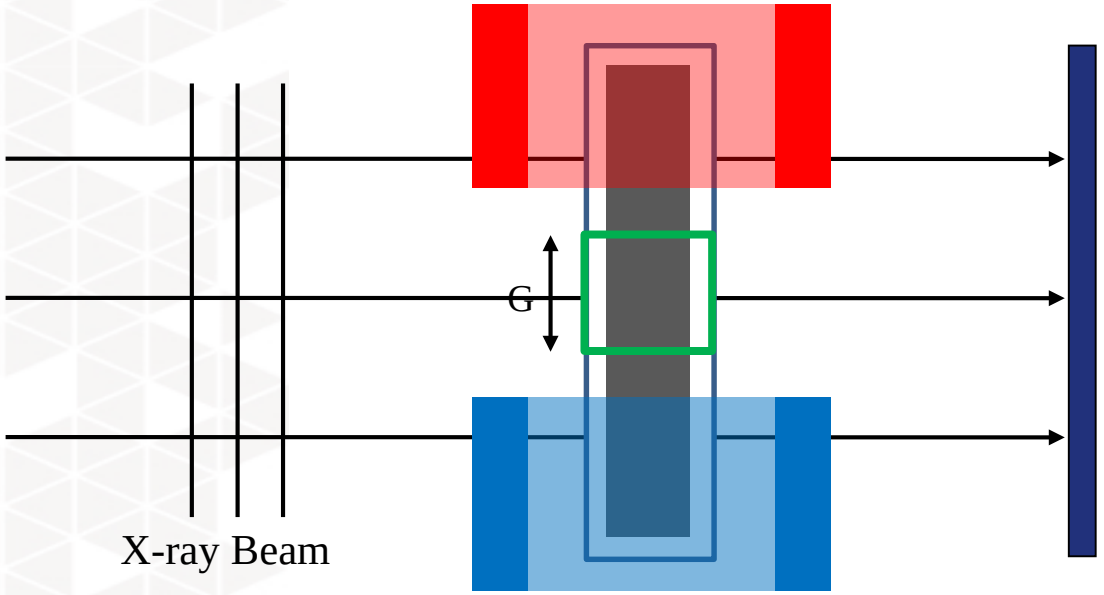

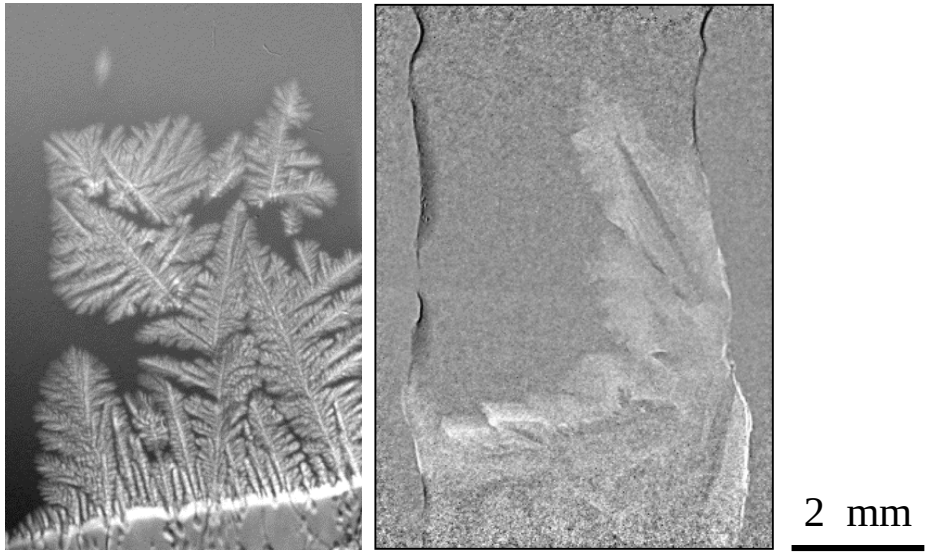

Contrast origin: **absorption** (Light elements or less dense → light grey. Heavy elements or denser → dark grey):

- **Metallic alloys**: atomic number
- **Silicon:** liquid and solid densities: $\rho_s = 2.31$ g.cm^{-3}, $\rho_l = 2.56$ g.cm^{-3}

Direct and non deformed image of the **solidification** (micro)structure ***in situ*** and **real-time**: **morphology, dynamics.**

X-ray Bragg diffraction imaging / X-ray Topography

- **1912** : First X-ray diffraction by a crystal (**Max von Laue, Friedrich & Knipping**)

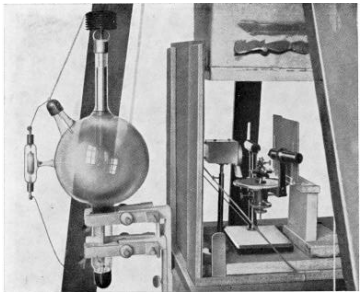

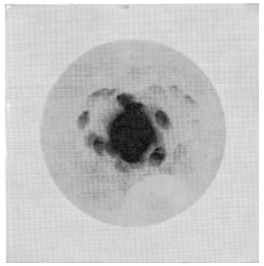

Copper sulfate

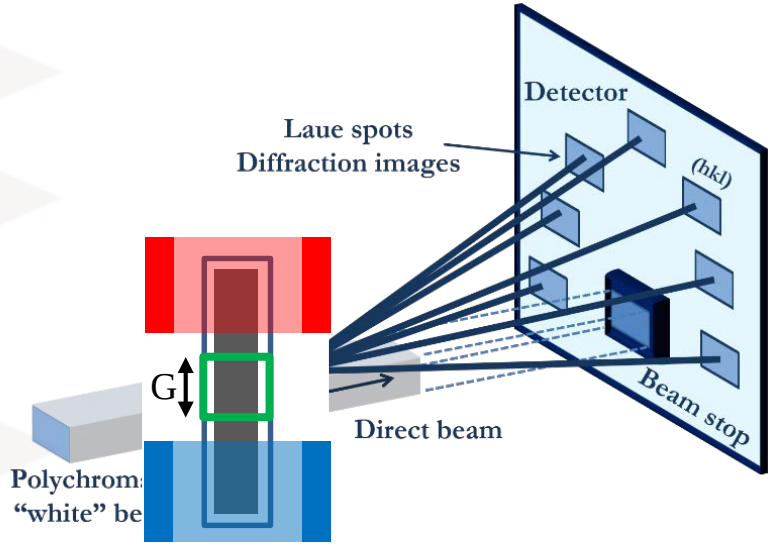

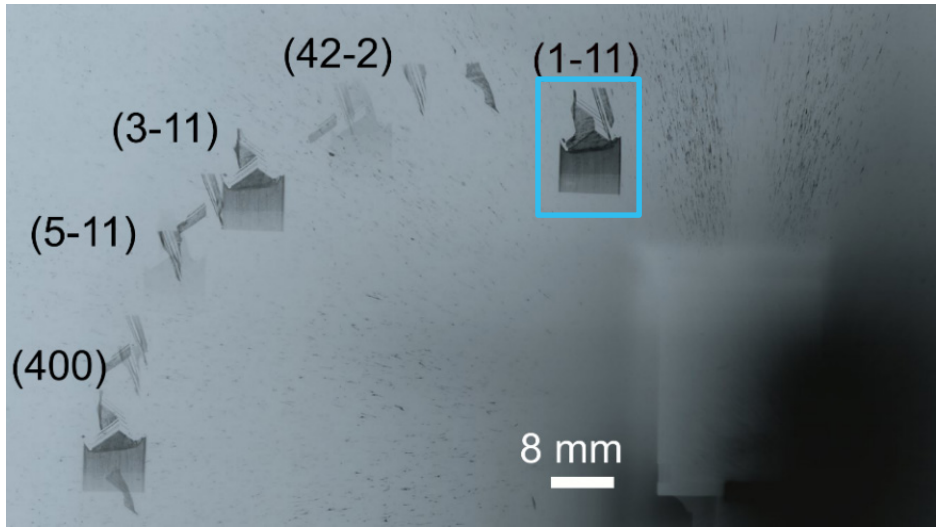

X-ray Bragg diffraction imaging / X-X-ray Topography

Becker et al., Journal of Applied Crystallography 52 (2019) 1312-1320.
&
Neves Dias et al., Phys. Status Solidi B (2022), 2100594

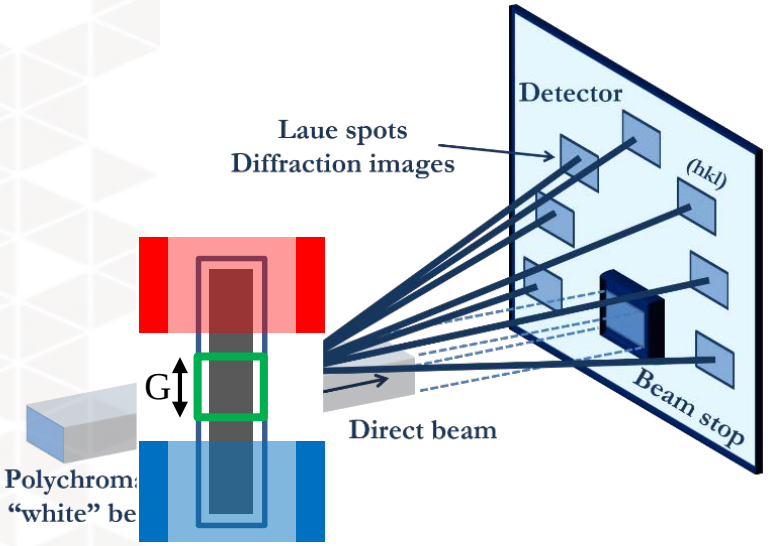

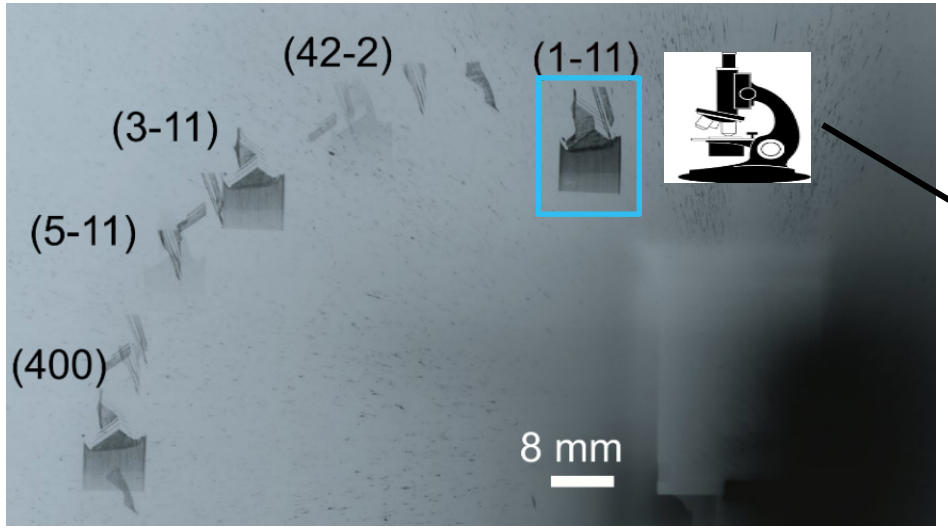

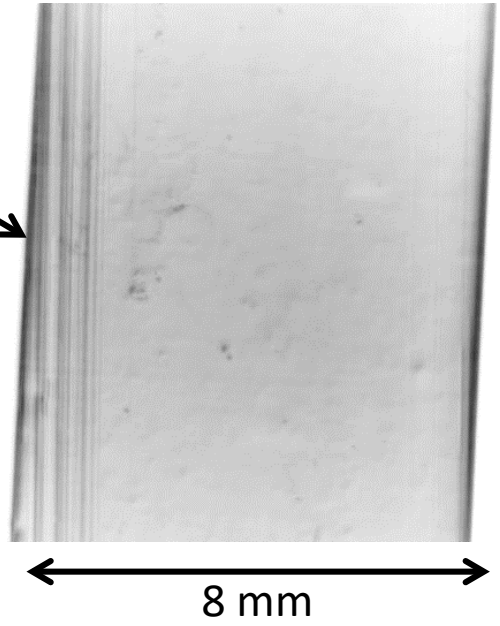

Bragg diffraction imaging:

- Spot position (Bragg law) ⇔ **Crystallographic orientation**
- Contrast ⇔ **Crystal lattice deformation, defects**

Deformed image of the **solidification** (micro)structure: **Crystallographic orientation, strains, defects and misorientations**

Simultaneous radiography and topography

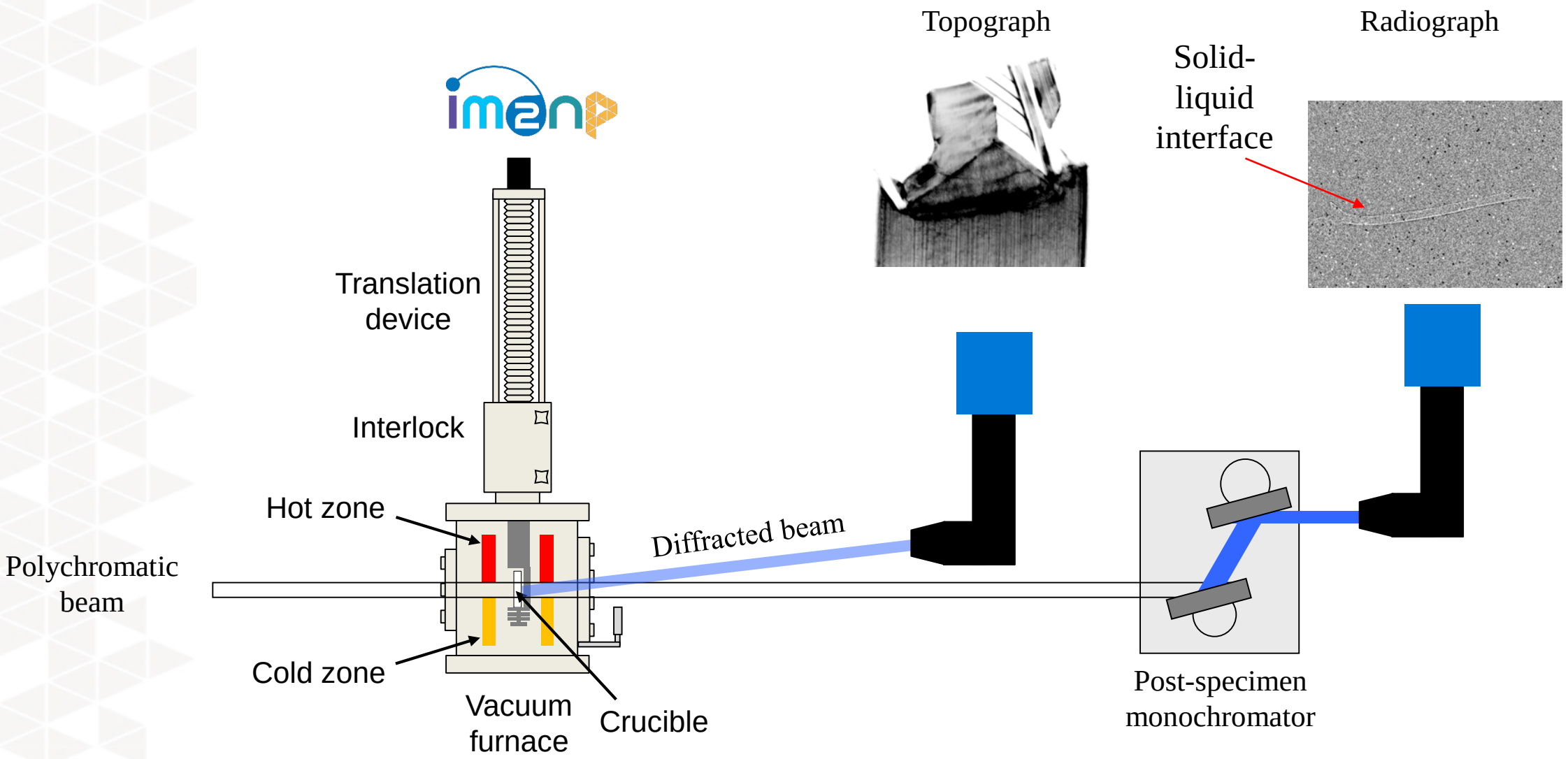

Another X-ray diffraction method: Rocking Curve Imaging

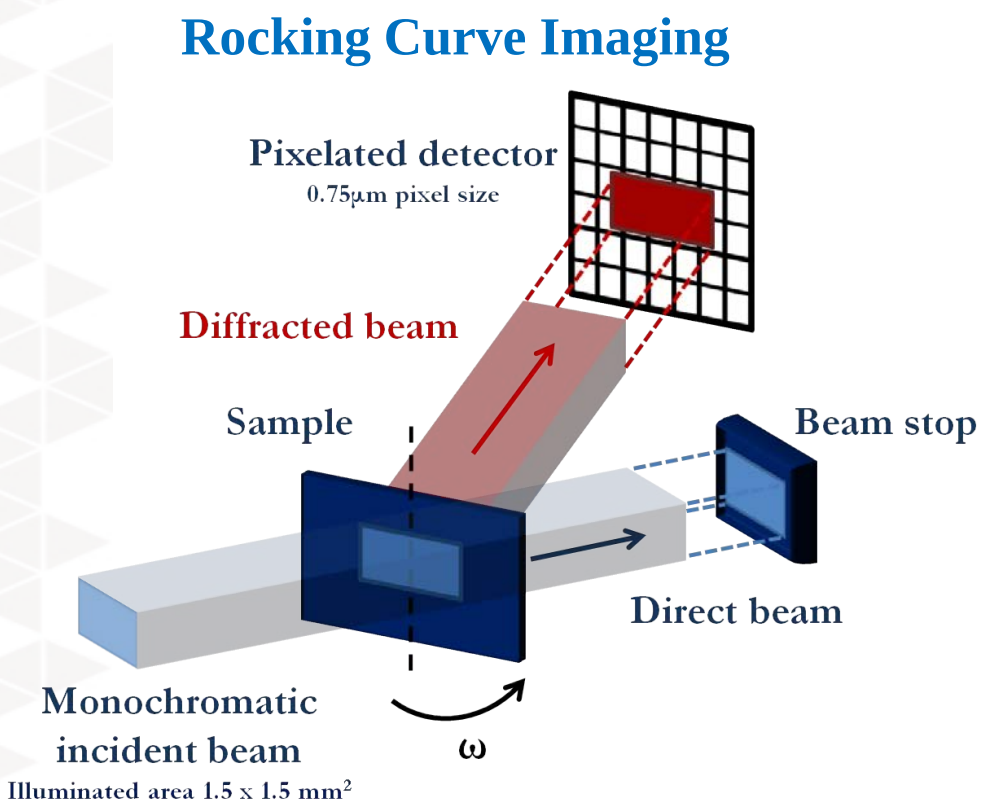

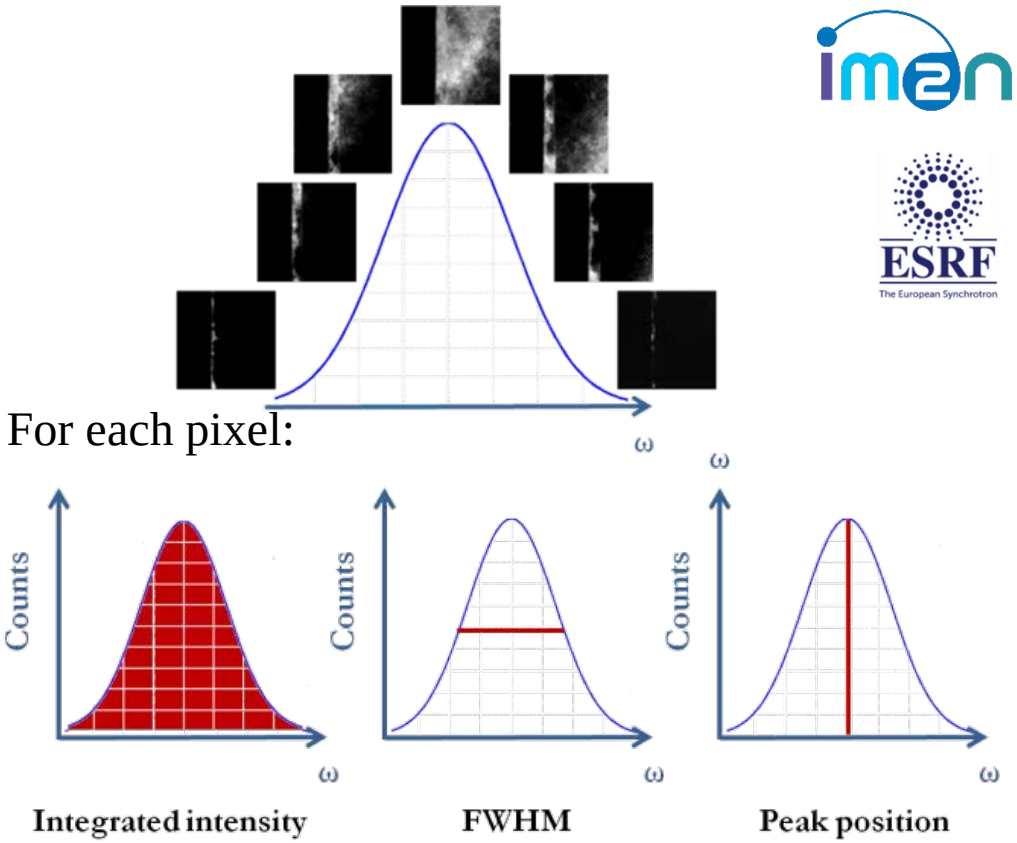

- Selection of a **single diffraction spot** (family of crystallographic planes).
- **Rocking curve** around the Bragg angle.

Provides quantitative information about:

- **Crystal perfection.**
- Level of **local distortion** (FWHM)
- **Rotation of crystal lattice** (PP)

Another X-ray diffraction method: Rocking Curve Imaging

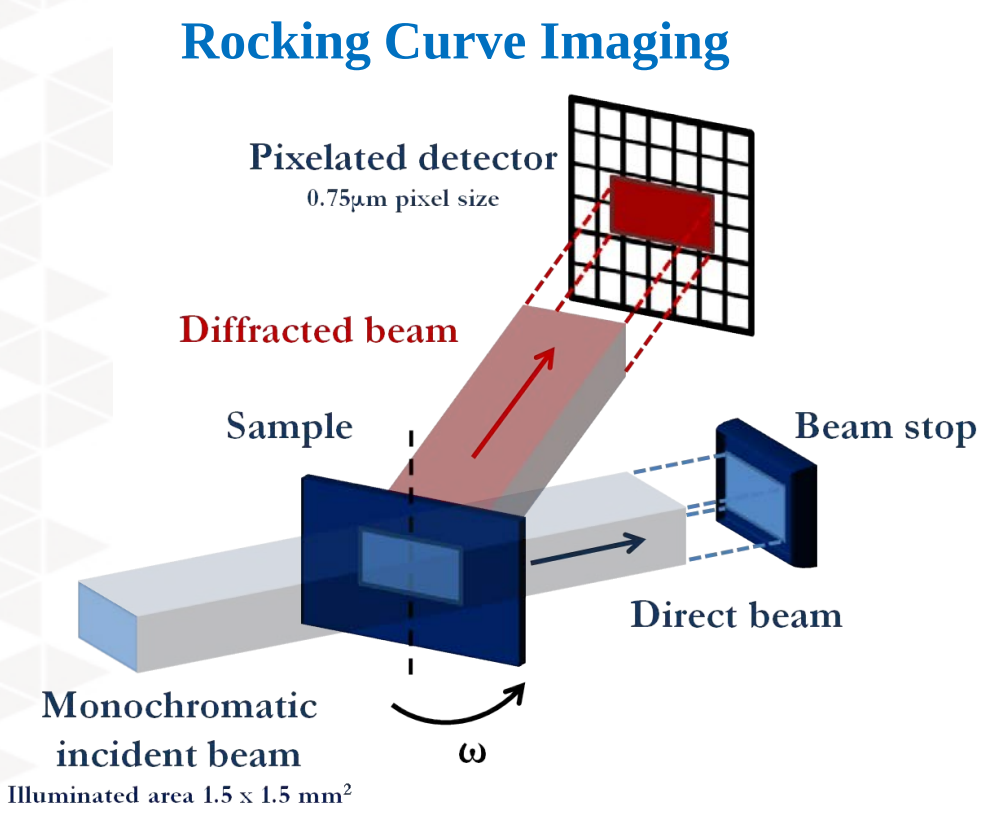

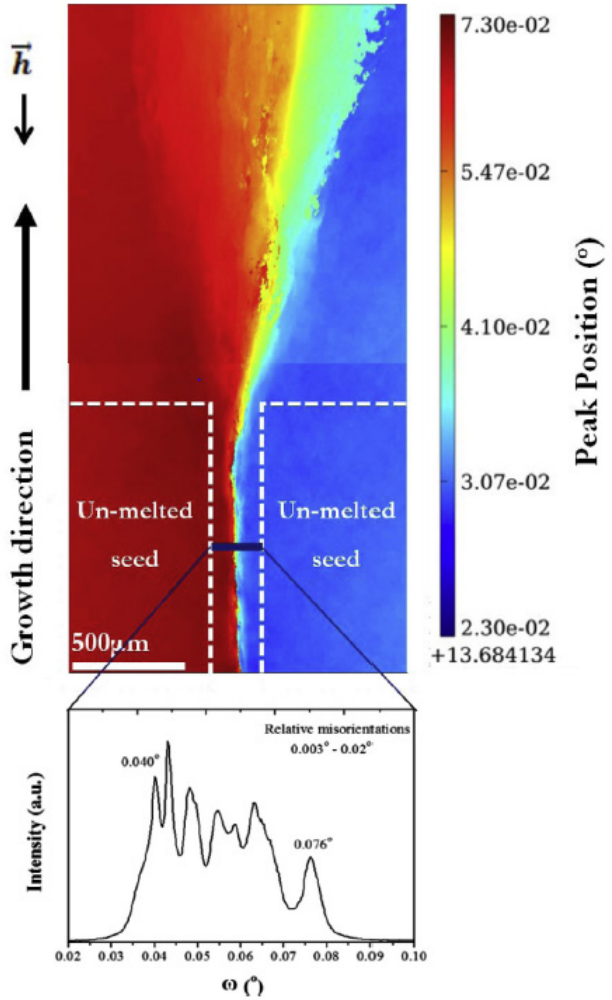

- Selection of a **single diffraction spot** (family of crystallographic planes).
- **Rocking curve** around the Bragg angle.

M.G. Tsoutsouva, Acta Materialia 88 (2015) 112–120

Electron Backscatter Diffraction - EBSD

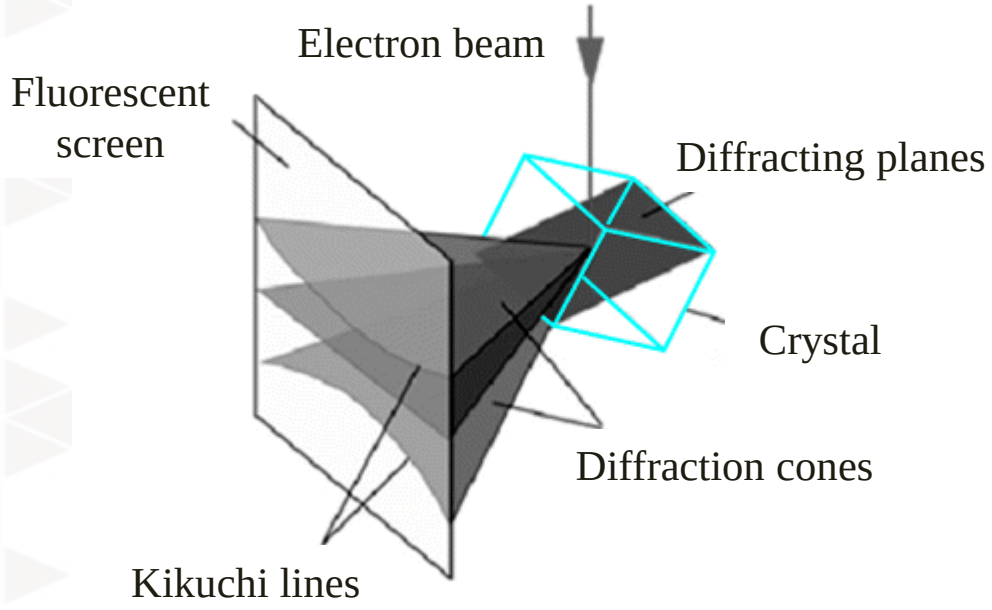

Kikuchi lines

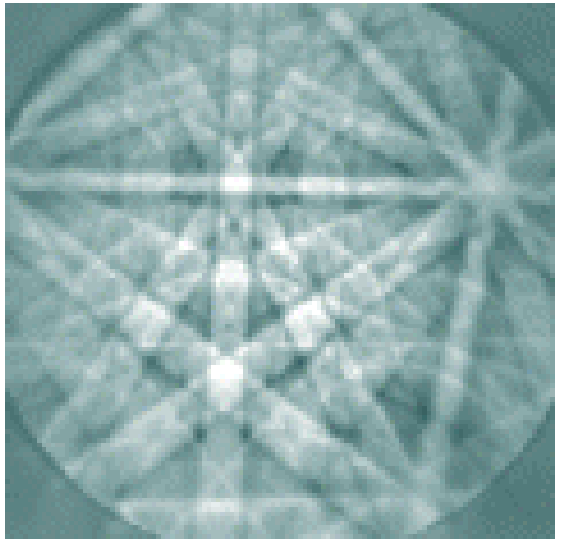

- Electron beam towards the sample → different families of atomic planes that are in **Bragg condition** → **backscattered electrons**.
- Backscattered electrons form two **widely open diffraction cones** → Kossel cones.
- Intersection of the Kossel cones with the fluorescent screen → **Kikuchi lines**, visible as bands.
- **Indexing** is done automatically by using algorithms through Hough transformation.

EBSD - Conditions

- **Microscope: EG JEOL JSM 7001F**
  - Acceleration voltage: 20 kV.
  - Working distance: 20 mm.
  - Tilt: 70°.
  - 'dynamic focus' active.
  - Magnification: x100.
  - Diaphragm of the objective: 50 µm.
  - 'probe current number‘: 16.
- **EBSD**
  - Camera: HKL Nordlys.
  - Camera resolution:1344 x 1024 pix² with a 4x4 binning for maps and no binning for the cross correlation method.
  - Minimum time per frame: 10 ms.
  - Averaging 4.
  - Camera gain : low.
  - Resolution of the Hough space: 70 pix.
  - Detection of 8 bands.
  - Measurement step: **7 µm and 0.7 µm** for higher spatial resolution (square grid).
  - **Software: Channel5 / Oxford Instruments (mirror software at IM2NP).**

A first example

Riberi-Béridot et al., Acta Materialia 177 (2019) 141e150

In situ X-ray radiography and Bragg diffraction imaging

Solid-Liquid Interface

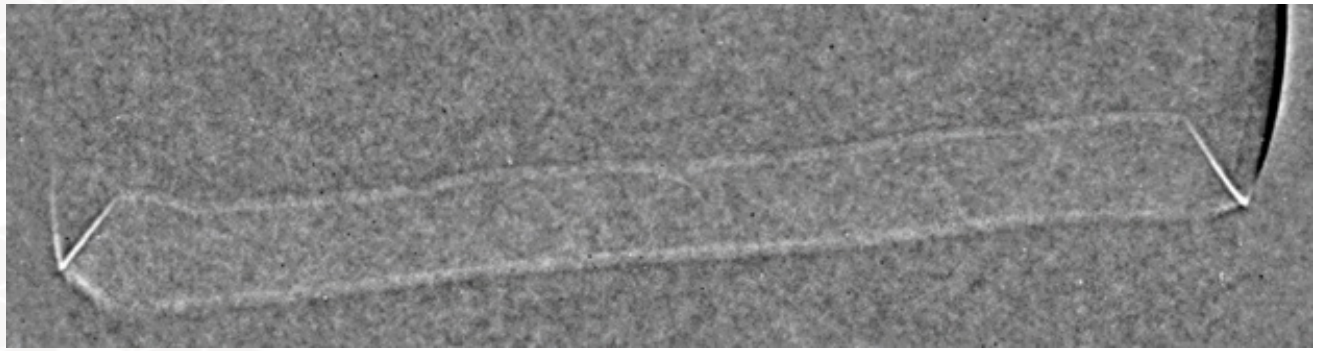

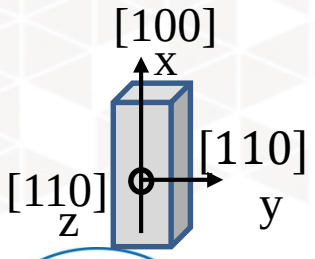

During solidification:
Applied temperature gradient: 30 K/cm.
Cooling rate of -1 K/min applied on both heaters at t_0.

In situ X-ray radiography and Bragg diffraction imaging

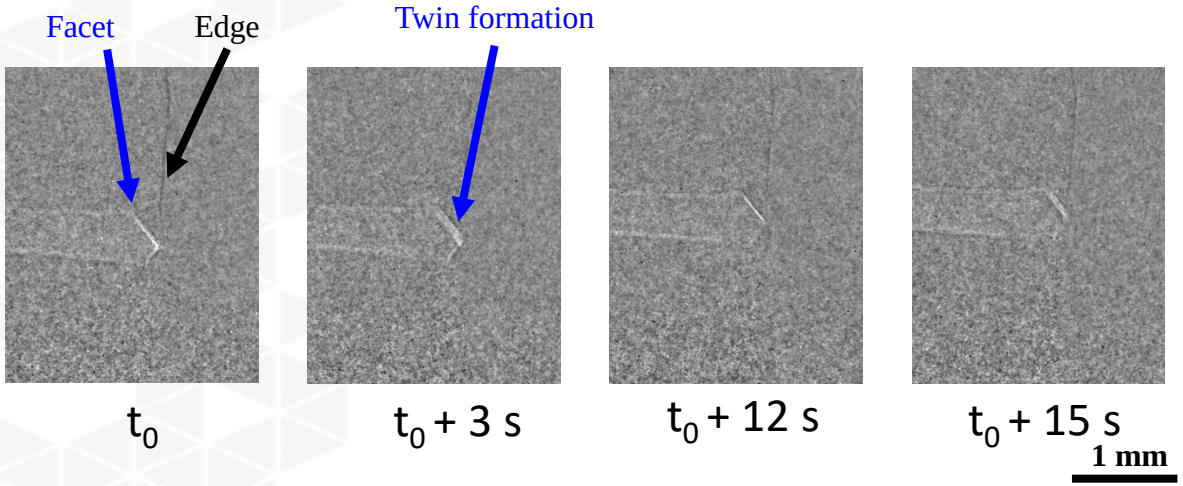

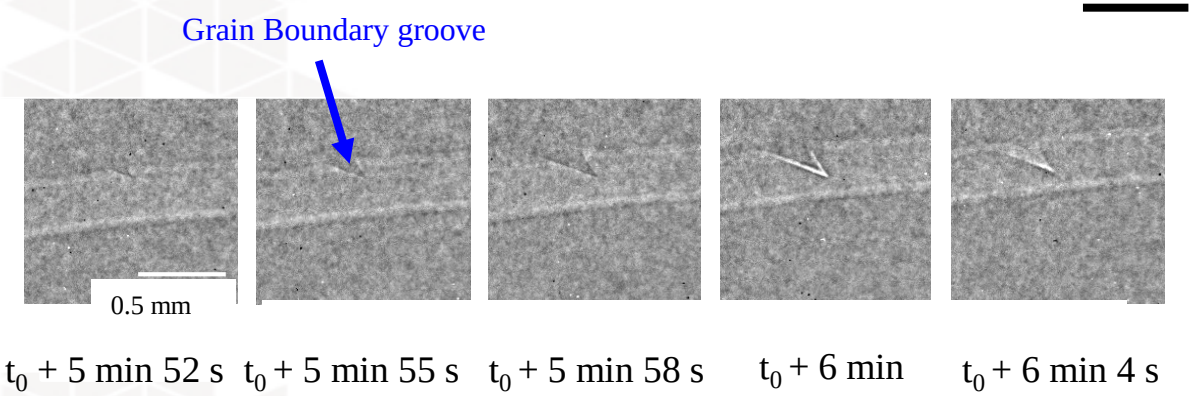

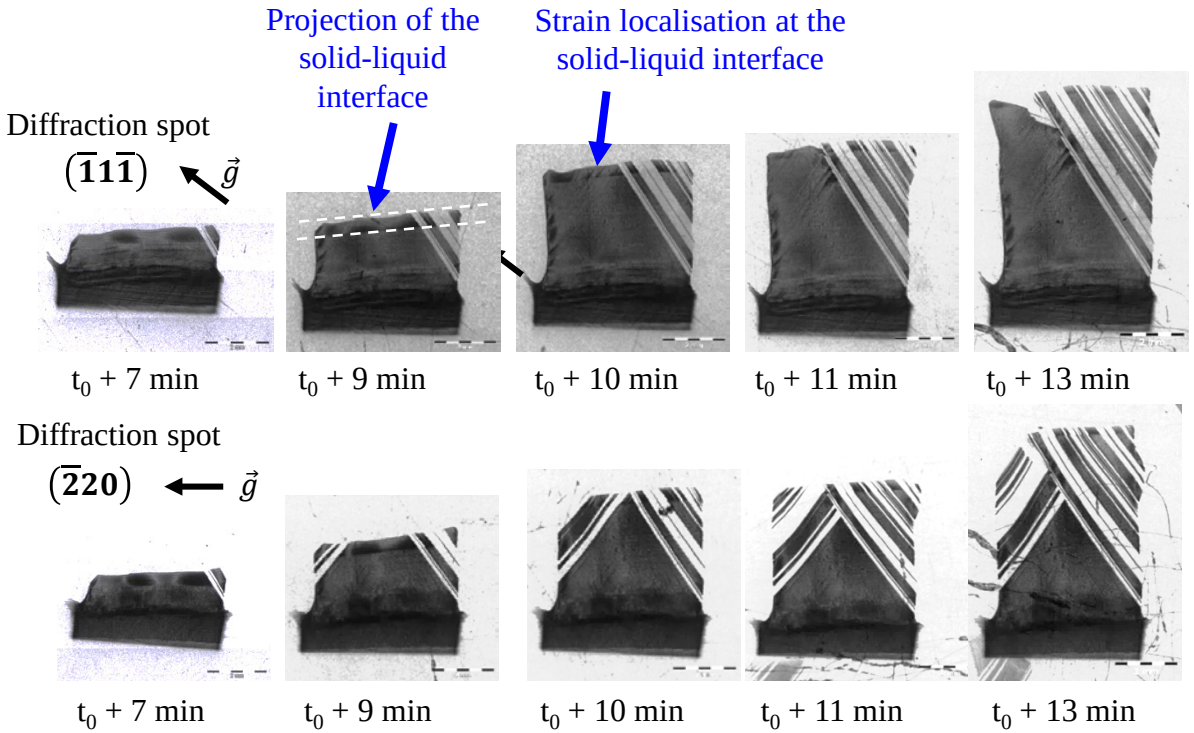

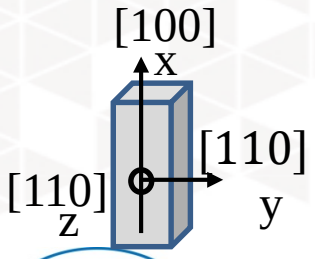

X-ray radiography

X-ray Bragg Diffraction Imaging

During solidification:

Applied temperature gradient: 30 K/cm.

Cooling rate of -1 K/min applied on both heaters at t_0.

EBSD results – IPF / CSL maps

Oxford Channel 5 software

IPFX – Growth direction

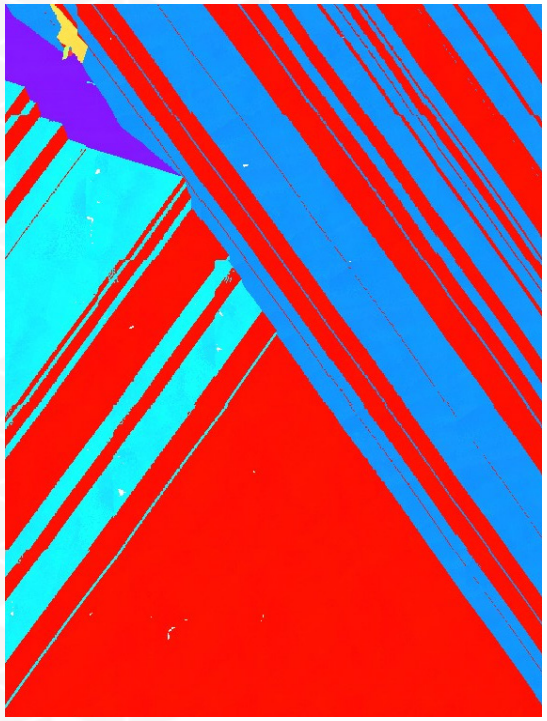

IPFX – Transverse direction

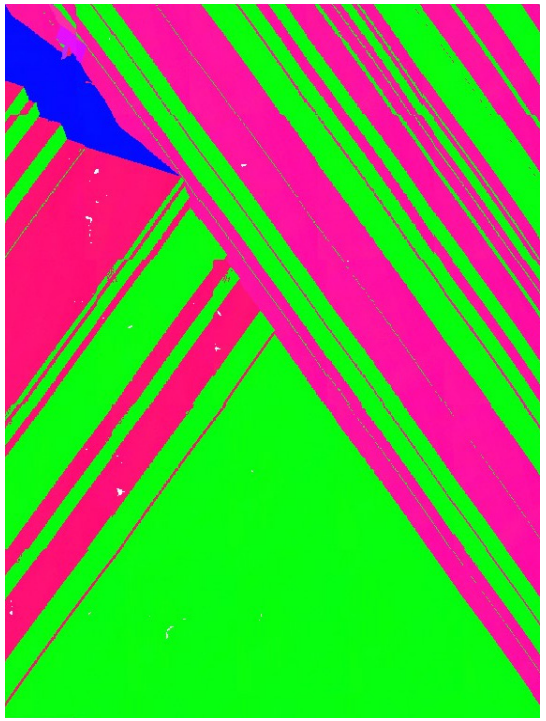

IPFZ – Normal direction

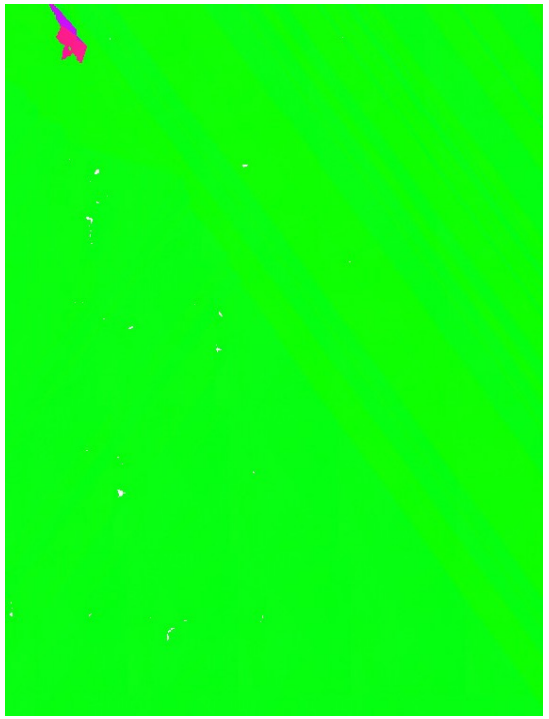

CSL – Coincidence site lattice map

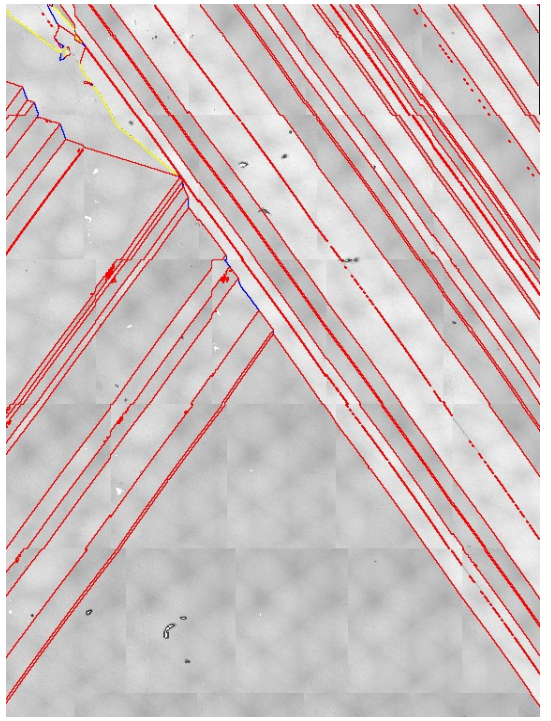

1 mm

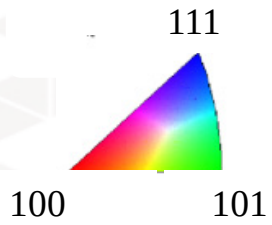

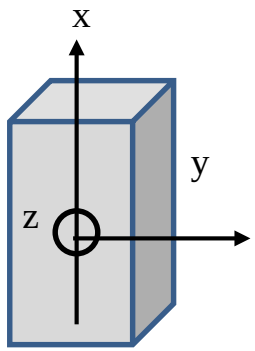

Twin boundaries - CSL: Brandon criterion

Σ3 <111> (60 ± 8.66) °
Σ9 <110> (38.94 ± 5) °
Σ27a <110> (31.58 ± 2.89) °

Σ3
Σ9
Σ27

Grain growth and competition

IPF map along the growth direction

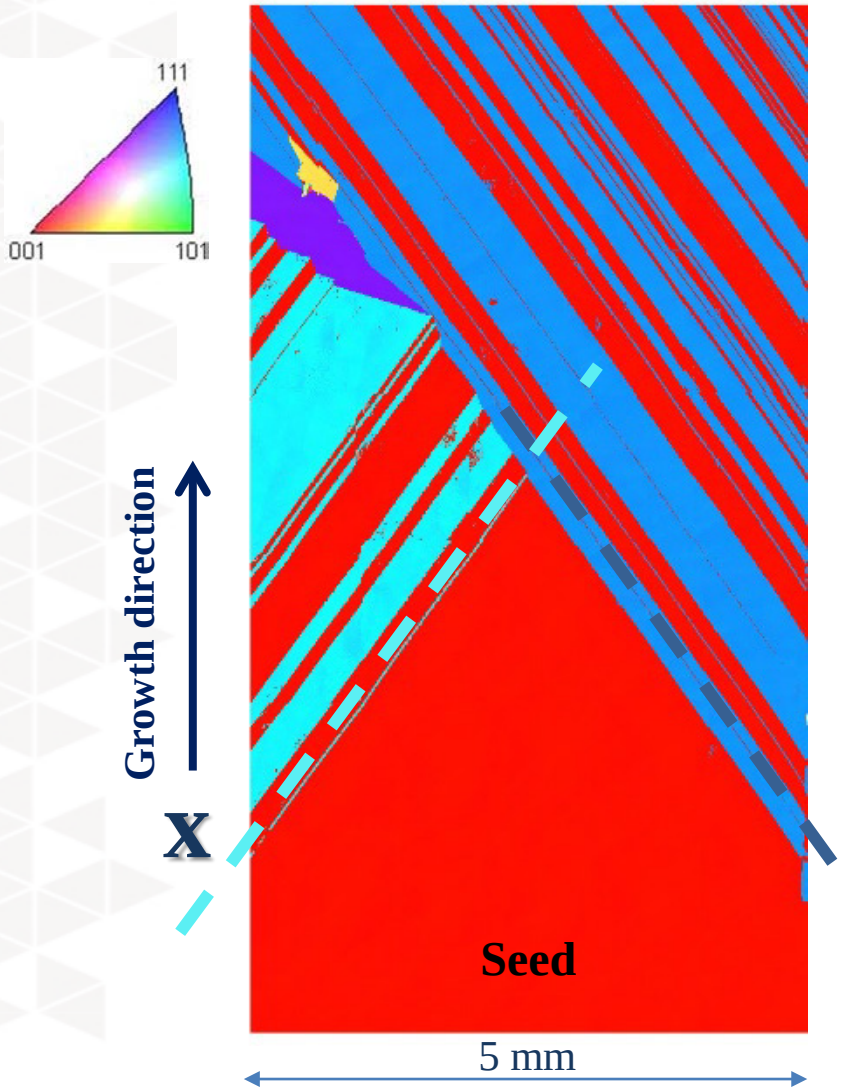

Radiography image of the facets at the edges

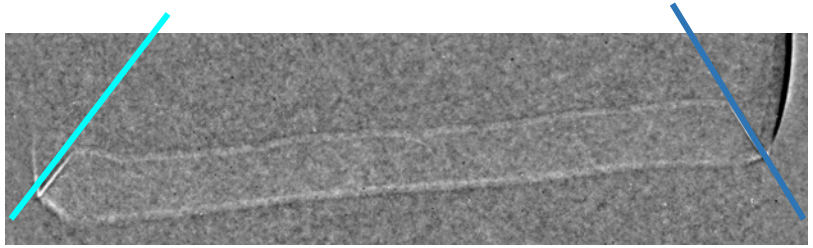

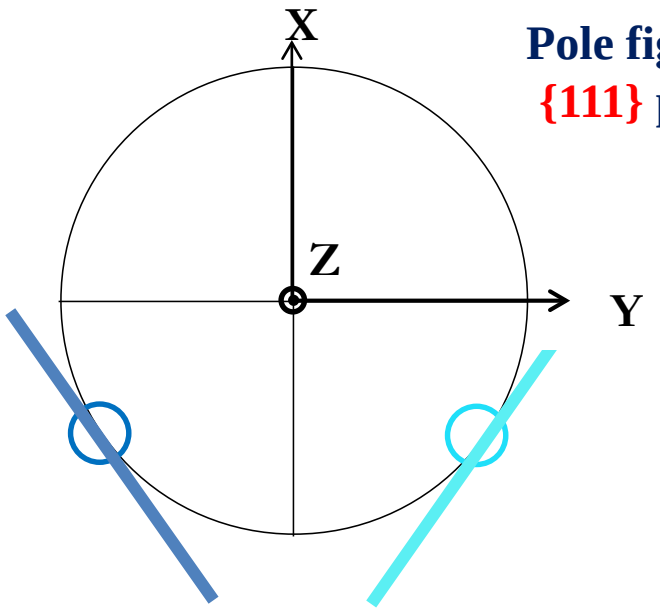

Pole figure of {111} planes

Riberi-Béridot et al. Acta Materialia 177 (2019) 141

Twinning / competition /deformation

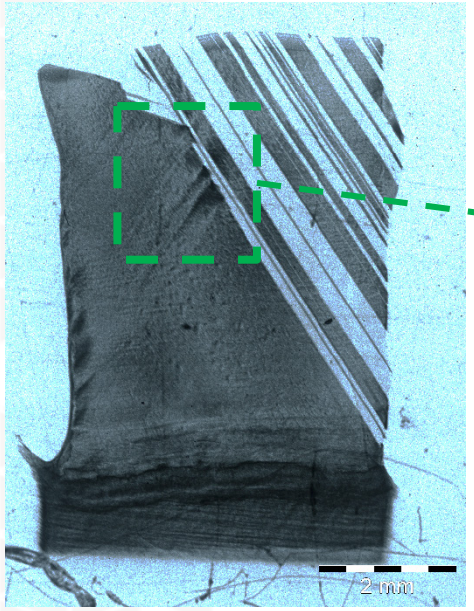

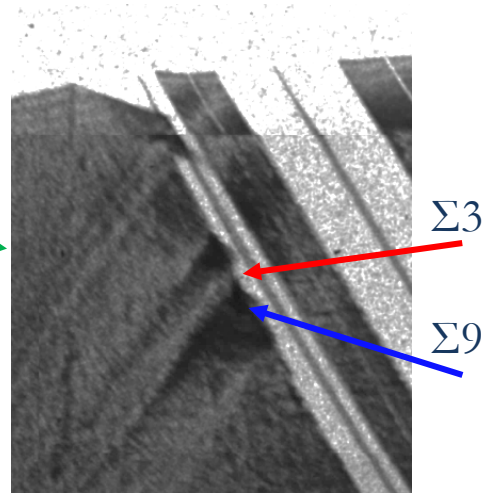

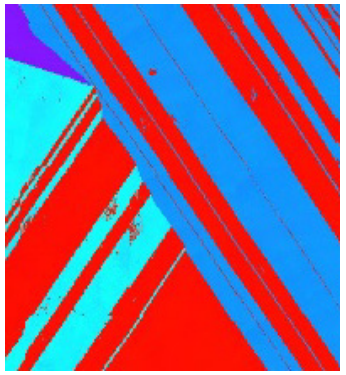

IPF X1 // growth direction

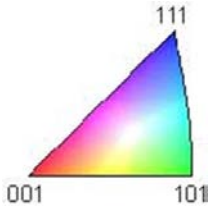

CSL (Coincidence Site Lattice)

Σ3
Σ9
Σ27

Σ=3	Σ=9	Σ=27a and b
$\{111\}_1/\{111\}_2$ - coherent 1st order twin boundary - most densely packed plane in the CSL	$\{122\}_1/\{122\}_2$ - 2nd order twin boundary - most densely packed plane in the CSL	$\{115\}_1/\{115\}_2$ - 3rd order twin boundary - most densely packed plane in the CSL
$\{112\}_1/\{112\}_2$ - incoherent 1st order twin boundary. -2nd most densely packed plane in the CSL	$\{114\}_1/\{114\}_2$ - 2nd order twin boundary -2nd most densely packed plane in the CSL	$\{552\}_1/\{552\}_2$ - 3rd order twin boundary -2nd most densely packed plane in the CSL
	$\{111\}_1/\{115\}_2$ - asymmetric 2nd order twin boundary -low density of coincidence sites	

Ervik et al. 26th Photovoltaic Solar Energy Conference

- **Strain field** at the **encounter of both twinned areas.**
- **Alternating contrast** depending on the twin boundary type.
- **Dislocation propagation**:
  - For Σ3 {111}/{111}: the two grains have a common {111} plane → direct cross.
  - For Σ9 {122}/{122}: accumulation and / or dislocation emission.

New grain nucleation

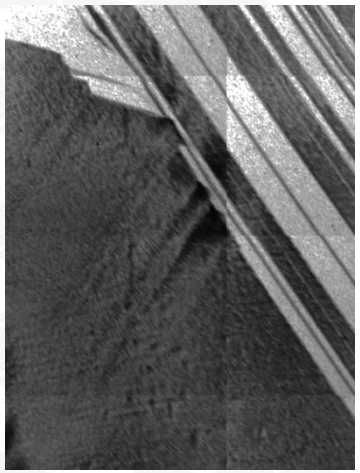

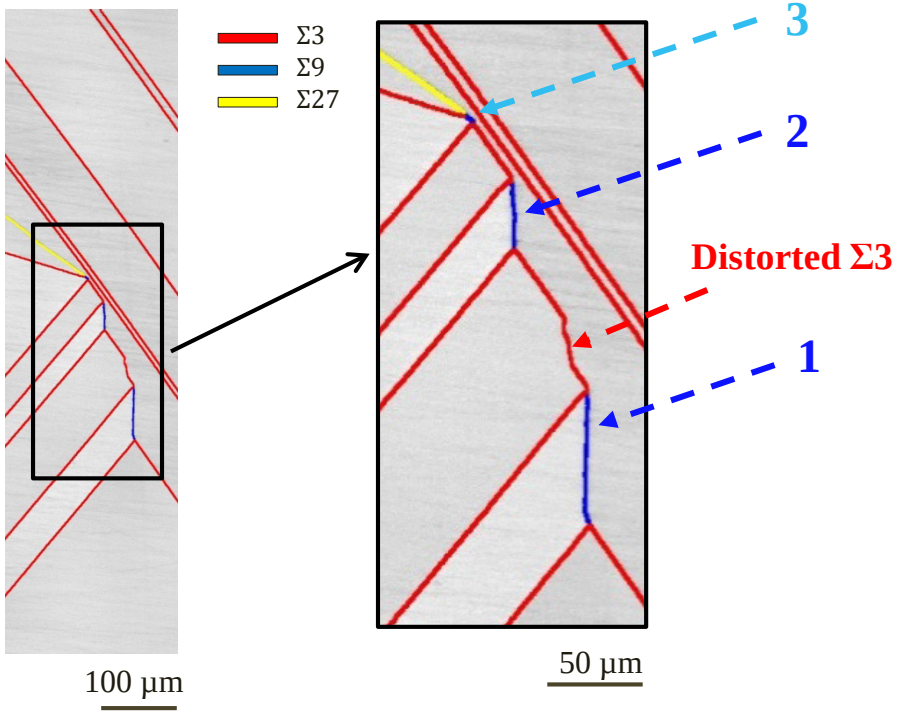

Pole figures and twin boundaries

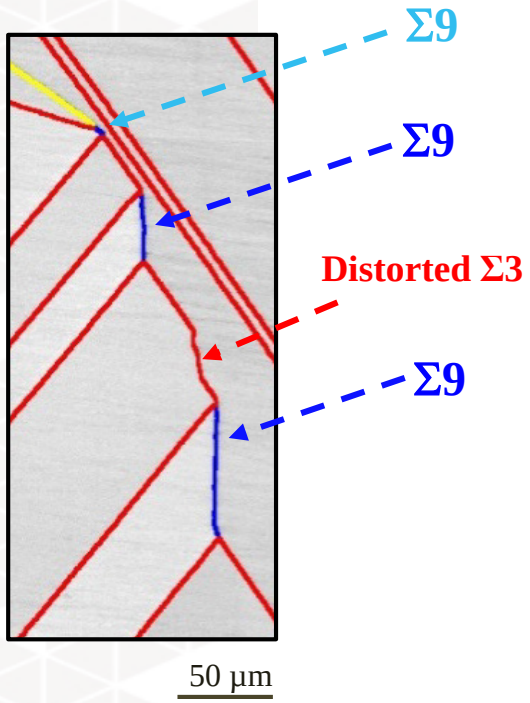

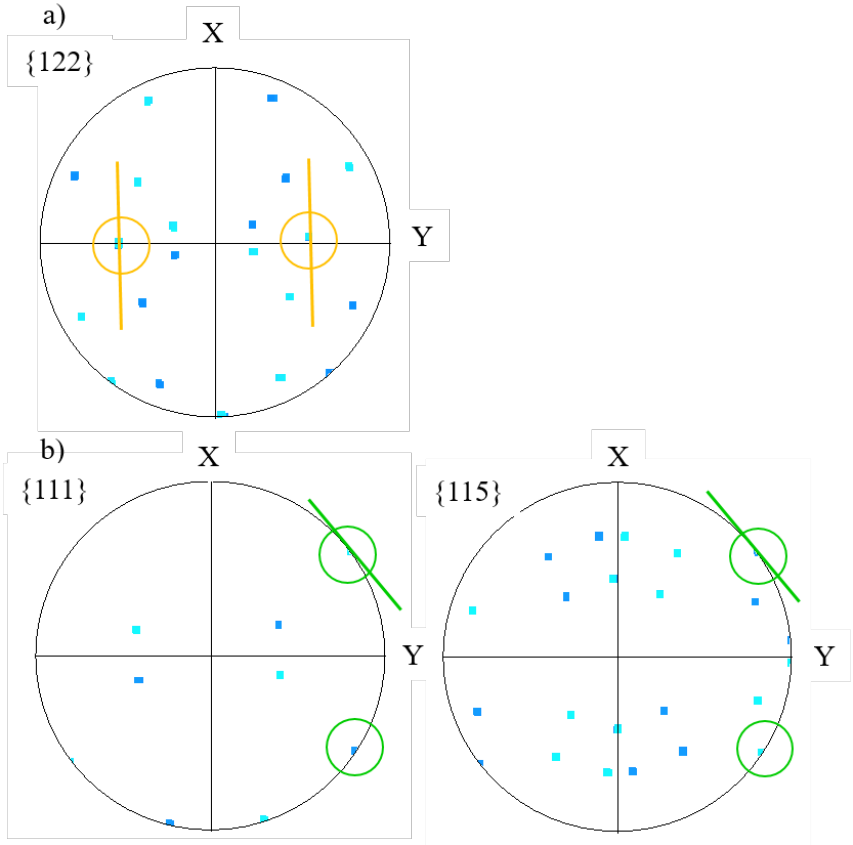

Σ=3	Σ=9	Σ=27a and b
$\{111\}_1/\{111\}_2$ - coherent 1st order twin boundary - most densely packed plane in the CSL	$\{122\}_1/\{122\}_2$ - 2nd order twin boundary - most densely packed plane in the CSL	$\{115\}_1/\{115\}_2$ - 3rd order twin boundary - most densely packed plane in the CSL
$\{112\}_1/\{112\}_2$ - incoherent 1st order twin boundary. -2nd most densely packed plane in the CSL	$\{114\}_1/\{114\}_2$ - 2nd order twin boundary -2nd most densely packed plane in the CSL	$\{552\}_1/\{552\}_2$ - 3rd order twin boundary -2nd most densely packed plane in the CSL
	$\{111\}_1/\{115\}_2$ - asymmetric 2nd order twin boundary -low density of coincidence sites	

Ervik et al. 26th Photovoltaic Solar Energy Conference

Two configurations of the **Σ9 twin boundaries** :

- Vertical grain boundary trace (orange lines) : Σ9 $\{122\}_{1,2}$ (Orange circle: common poles).
- Inclined grain boundary trace (green lines) : Σ9 $\{111\}_1/\{115\}_2$ (Green circles: common poles).

New grain nucleation

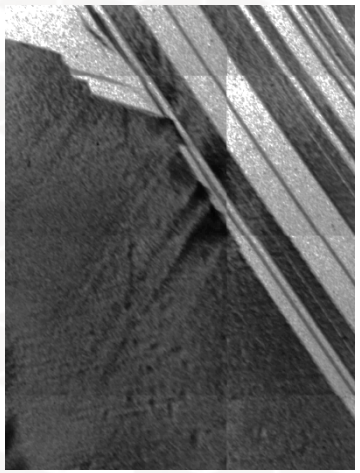

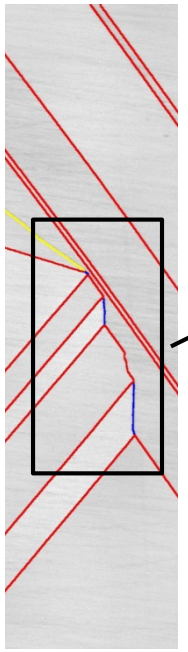

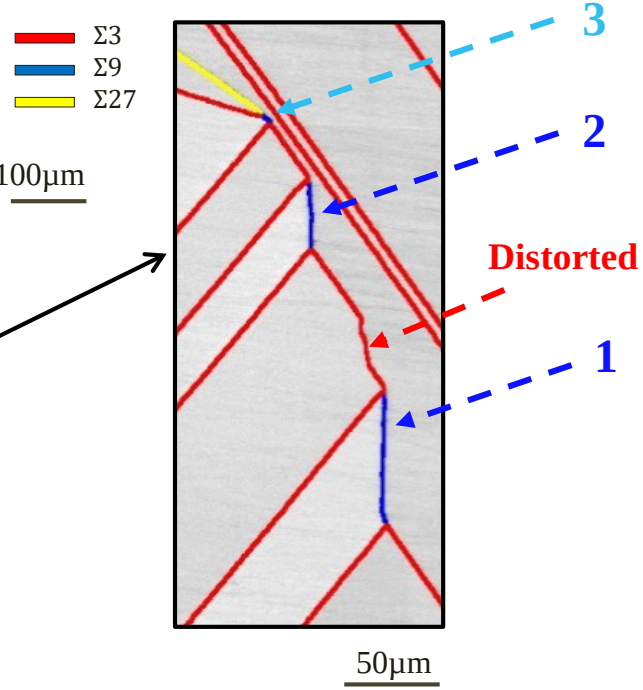

GOS (Grain Orientation Spread) *

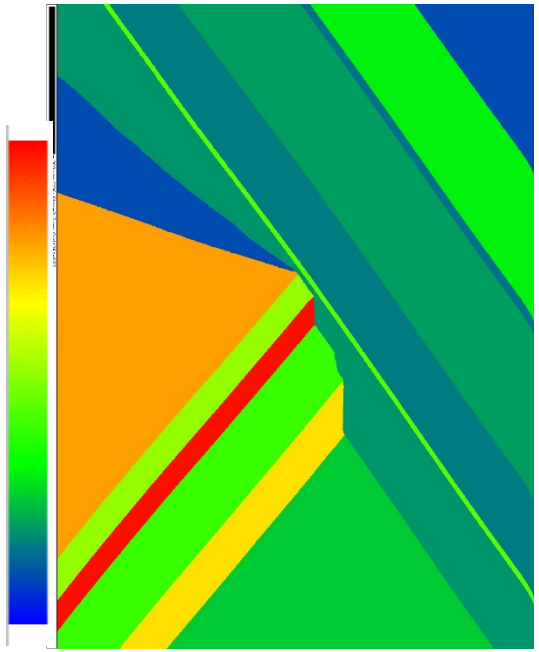

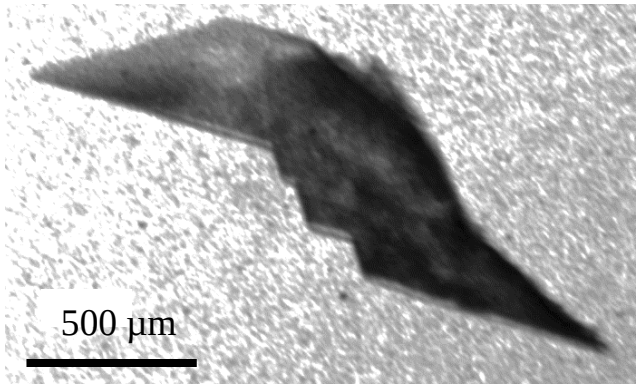

- **Σ9 <110> | {122}/{122} symmetric and coherent (1,2)** & aligned along the growth direction.
- **Σ9 <110> → no possible plane in common due to competition (3)** → Not energetically favourable conditions ⇒ **Nucleation of a new grain.**
- **Lower deformation level** after the new grain nucleation

* GOS: Average value of the difference between the orientation of each pixel in the grain and of the grain average orientation for each pixel. To evidence the distorted grains within a grain structure.

A second example

Not yet published

EBSD results – IPF / CSL maps

Oxford Channel 5 software

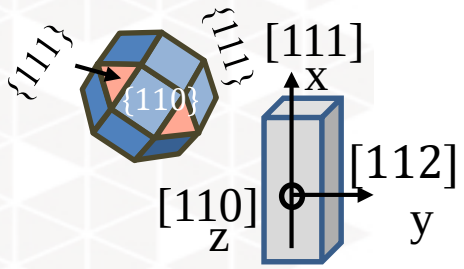

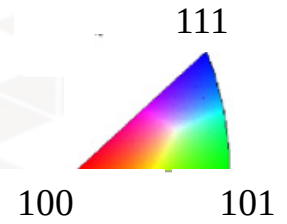

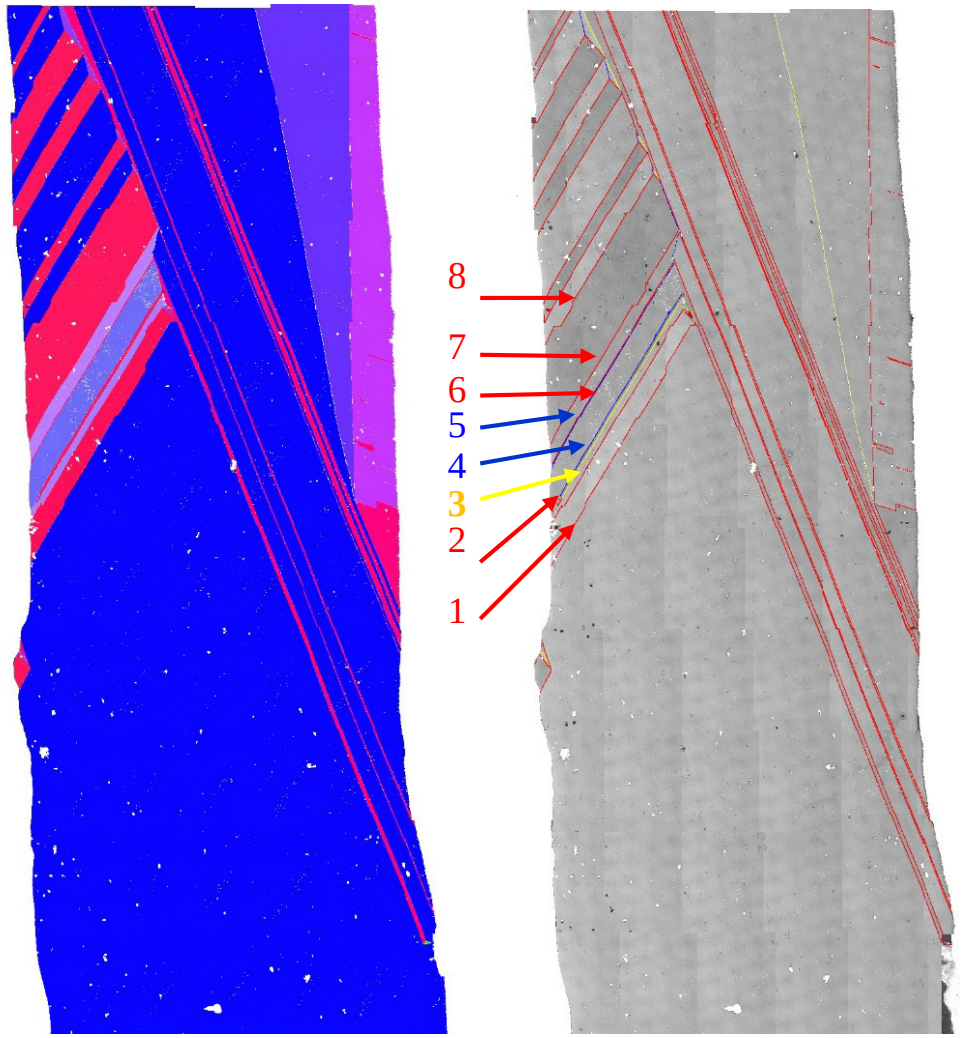

Zone melting sample with a **contamination in carbon (C): 1.5 10^{17} at/cm^3**

Twin boundaries - CSL: Brandon criterion

Σ3 <111> (60 ± 8.66) °
Σ9 <110> (38.94 ± 5) °
Σ27a <110> (31.58 ± 2.89) °

Σ3
Σ9
Σ27

EBSD results – IPF / CSL maps

Oxford Channel 5 software

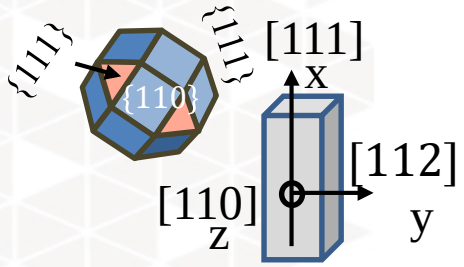

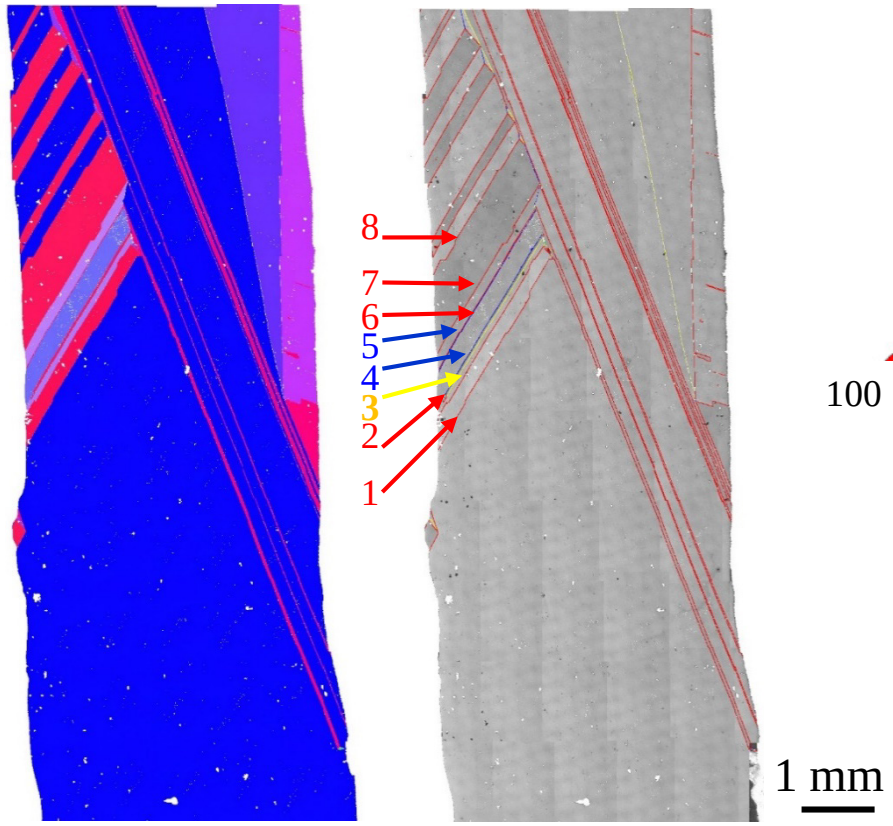

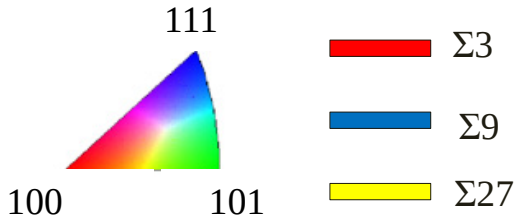

- Nucleation of **higher order twins**.
- Hypothesis: due to the **presence of C and SiC precipitates** (characterised by other methods).

Grain boundary types

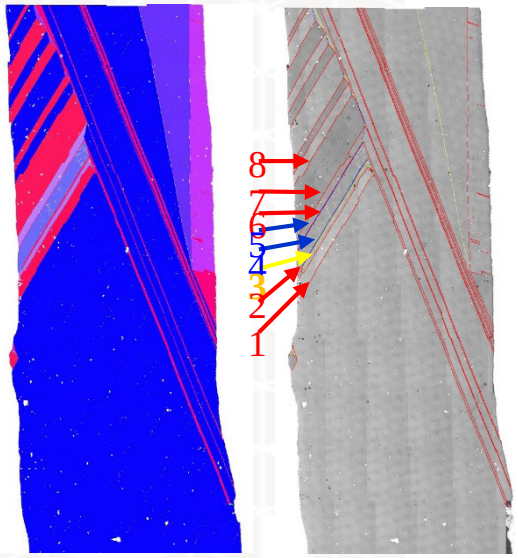

1 mm

- **1: Σ3** symmetrical {111} / {111}
- **2: Σ3** **symmetrical {112} / {112}**
- **3: Σ27** **symmetrical {115} / {115}**
- **4: Σ9** **symmetrical {114} / {114}**
- **5: Σ9** **symmetrical {114} / {114}**
- **6: Σ3** symmetrical {111} / {111}
- **7: Σ3** symmetrical {111} / {111}
- **8: Σ3** symmetrical {111} / {111}

Deformation of the twin boundaries corresponding to **unusual nucleation**

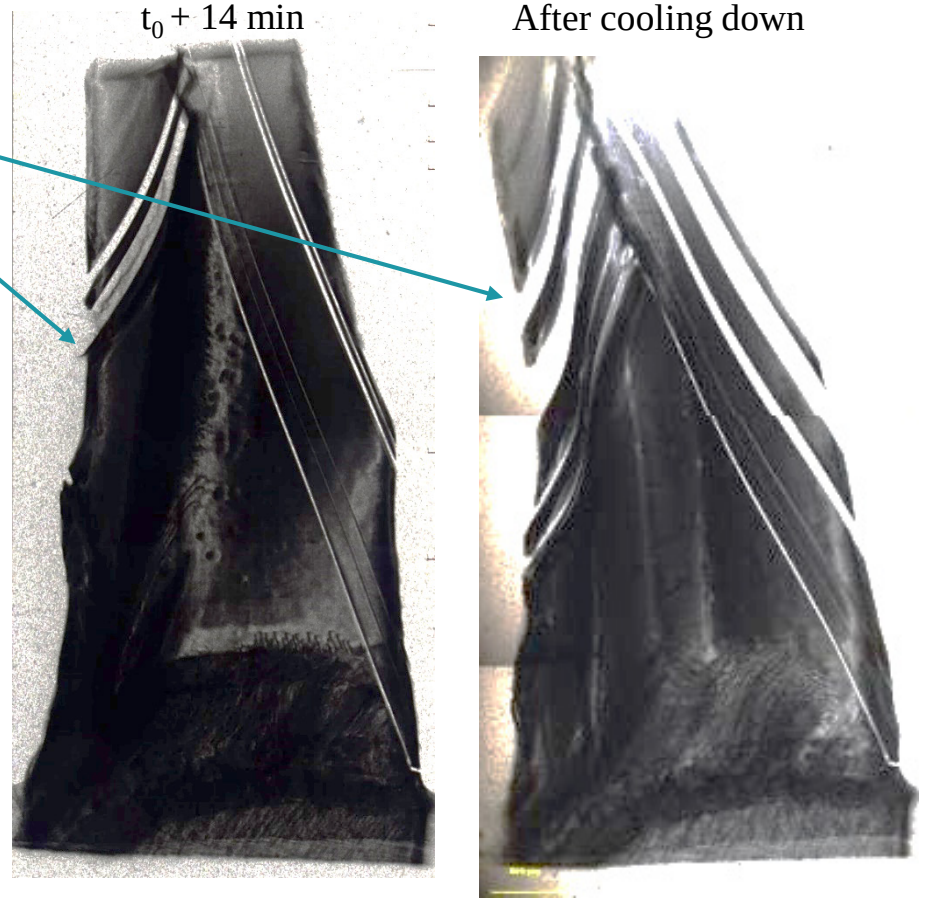

- Grain boundary characteristics from pole figures: **unusual twin boundary types** due to **nucleation** during solidification and not to competition.
- **Deformation** at the level of these twin boundaries.
- **This was never observed in pure samples !**

In situ Bragg diffraction imaging

X-ray Bragg Diffraction Imaging

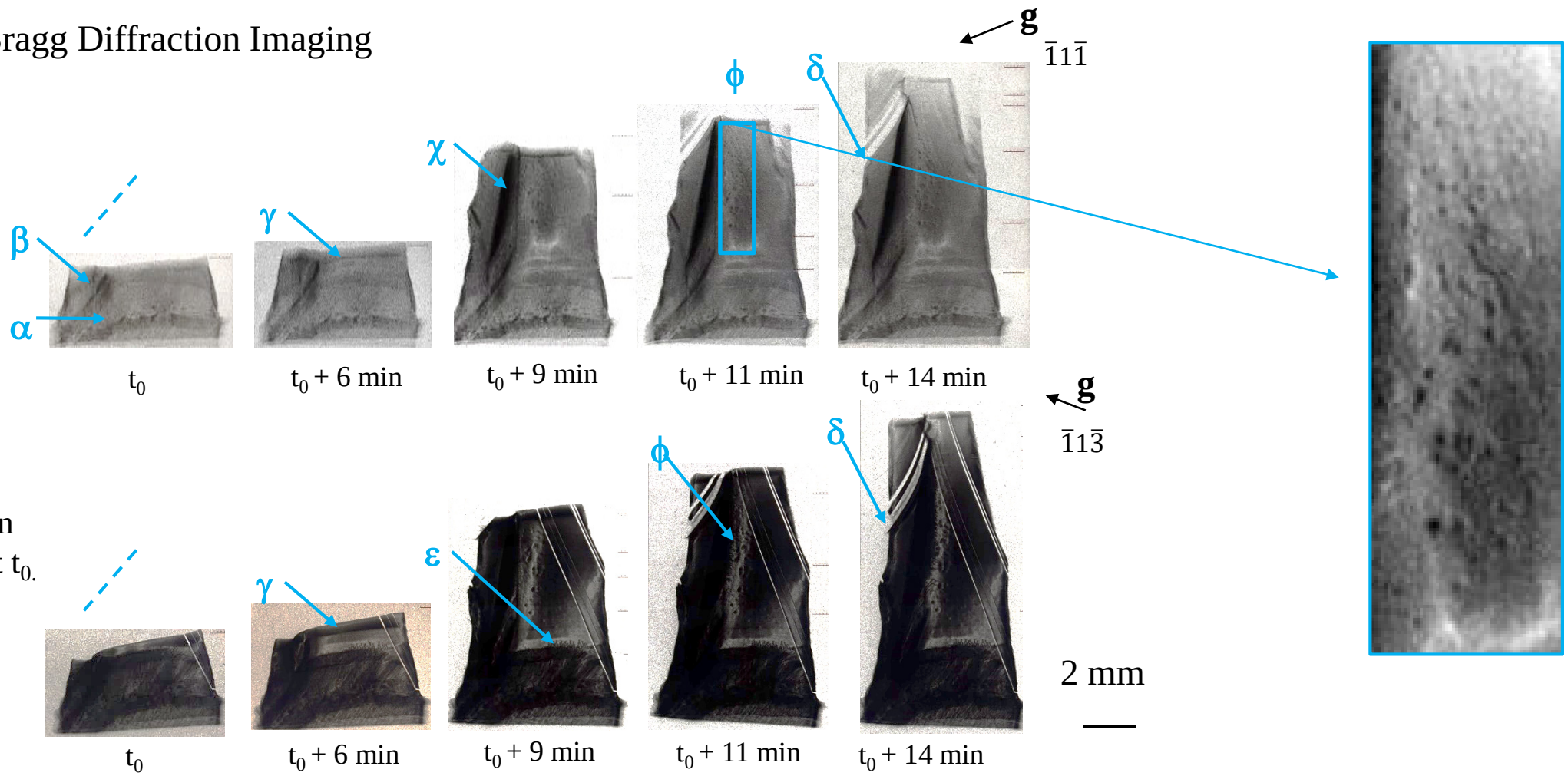

During solidification:
Applied temperature gradient: 31 K/cm.
Cooling rate of -1 K/min applied on both heaters at t_0.

Local deformation characterised by RCI – Projection mode

Full Width Half Maximum map

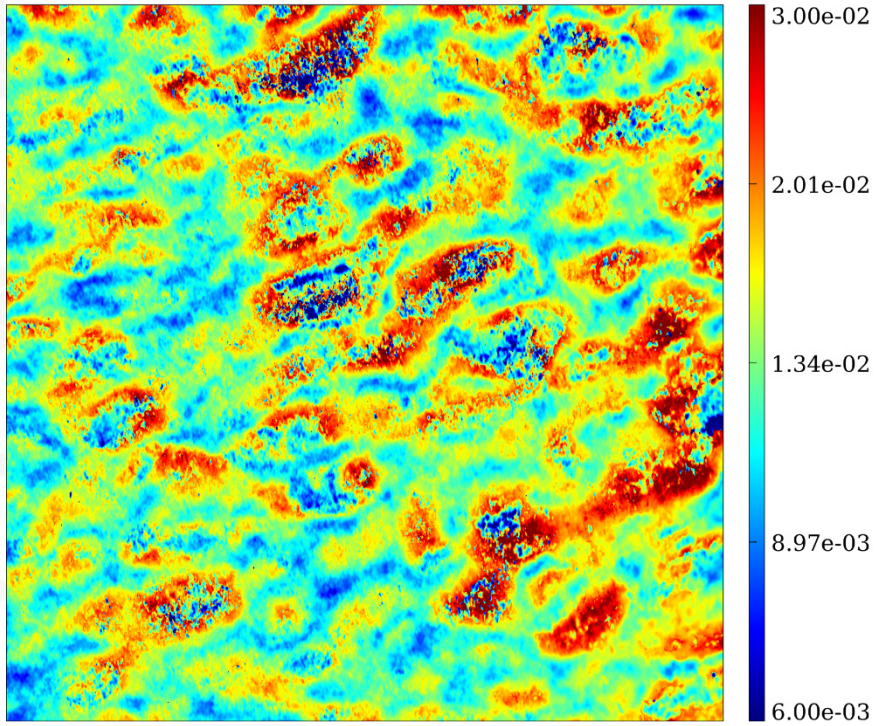

Peak-position map

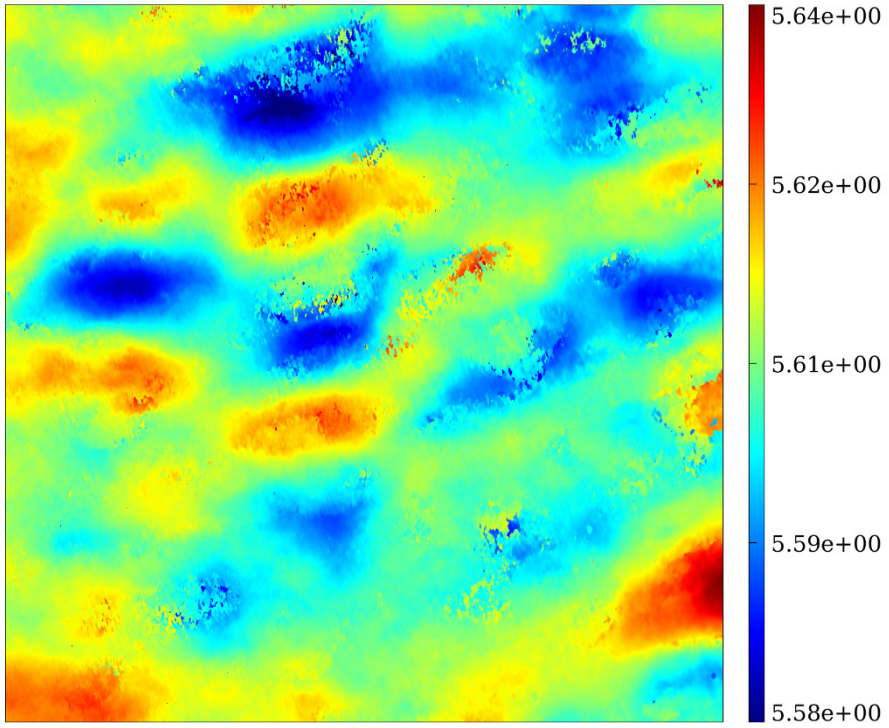

250 µm

- **Localized deformation** all over the sample.
- Corresponds to **small angle grain boundaries** (10^{-2} °).

Local deformation characterised by RCI – Section mode

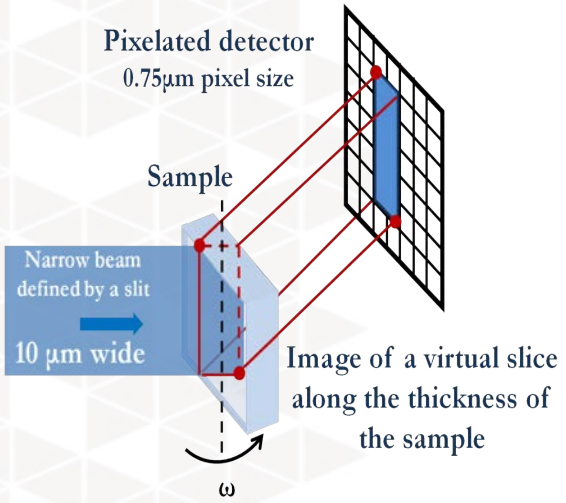

Full Width Half Maximum map

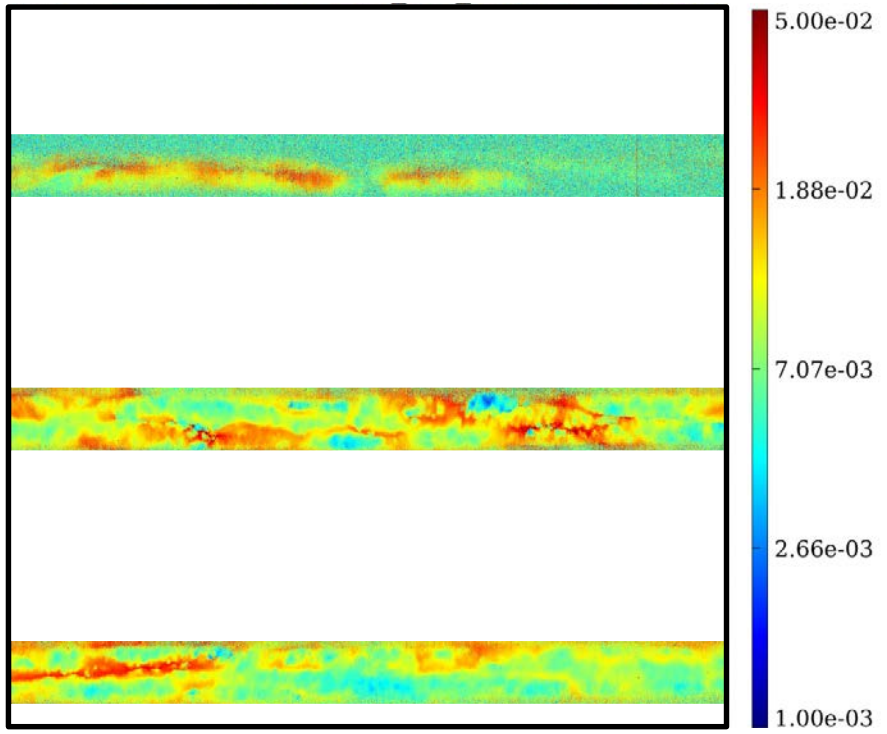

Peak-position map

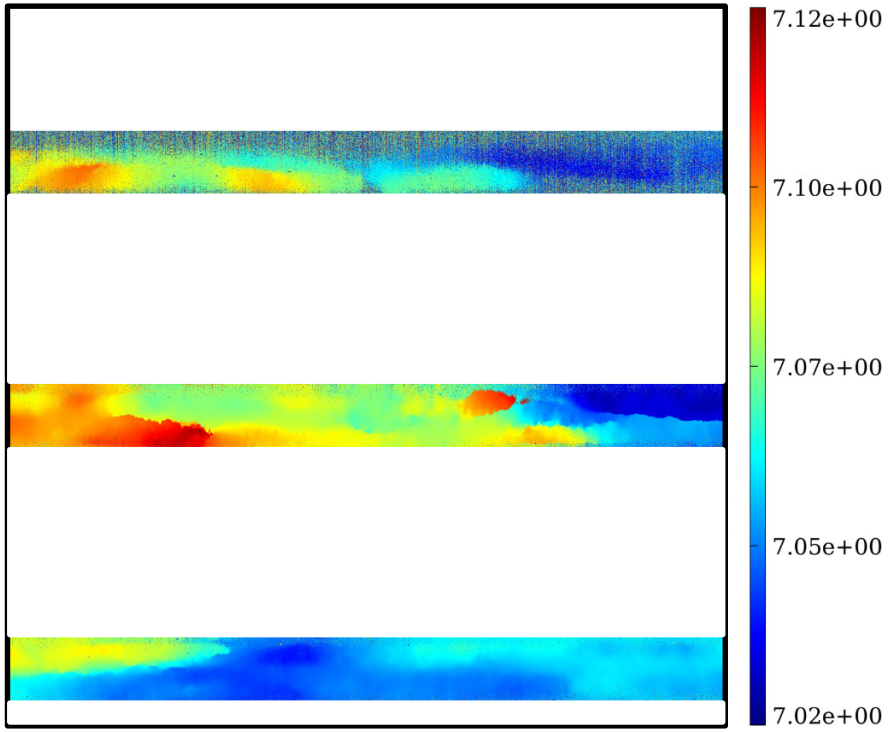

250 µm

- **Deformation** observed within the thickness of the sample : not a surface issue.
- Deformation of the crystal : 10^{-2} ° at the level of the local deformed areas.

Cross-correlation method

S11 stress

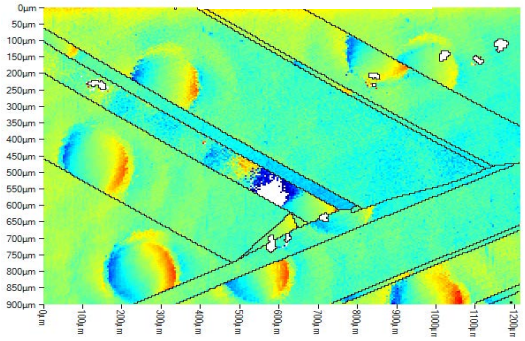

S12 stress

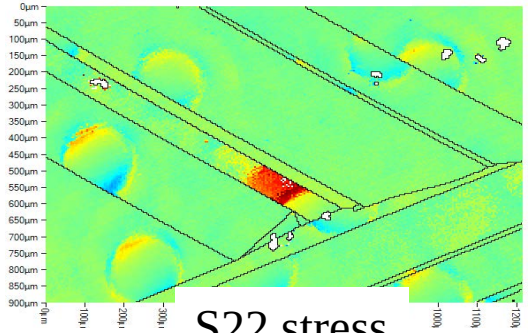

S31 stress

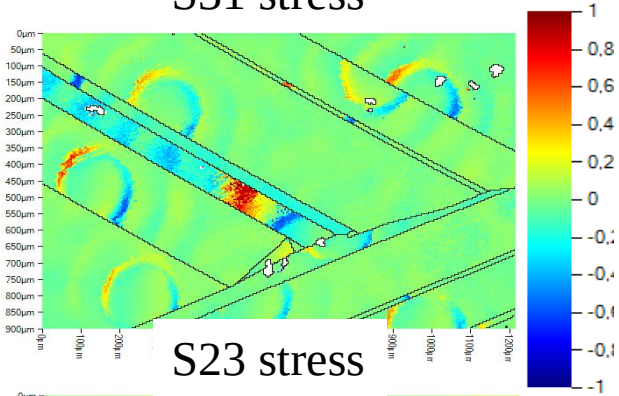

S22 stress

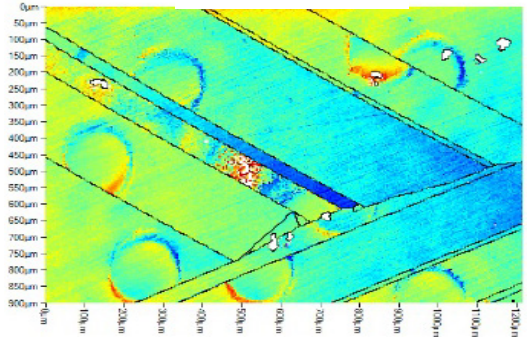

S23 stress

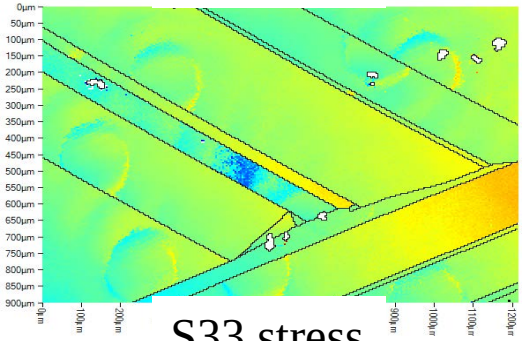

Solidification direction

Von Mises (GPa)

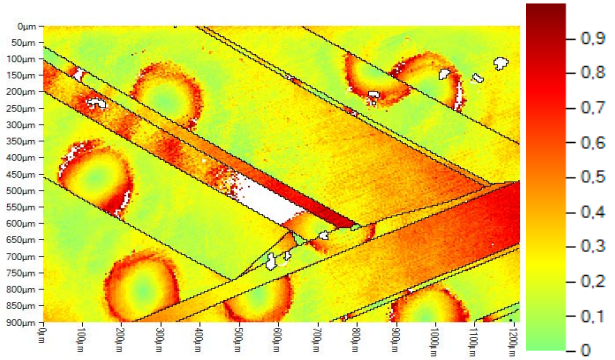

S33 stress

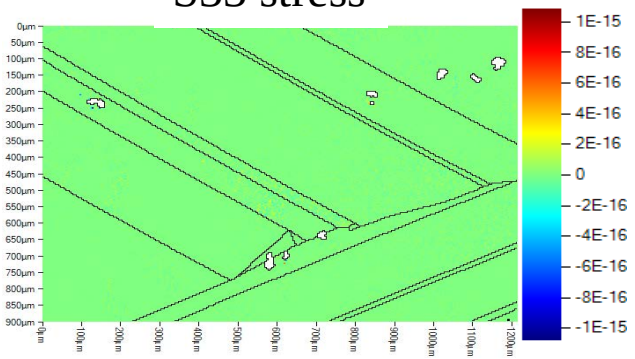

Comparison with cross-correlation method

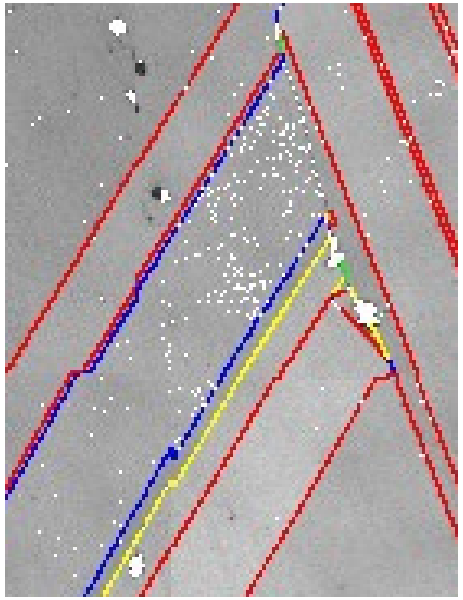

CSL map at the competition

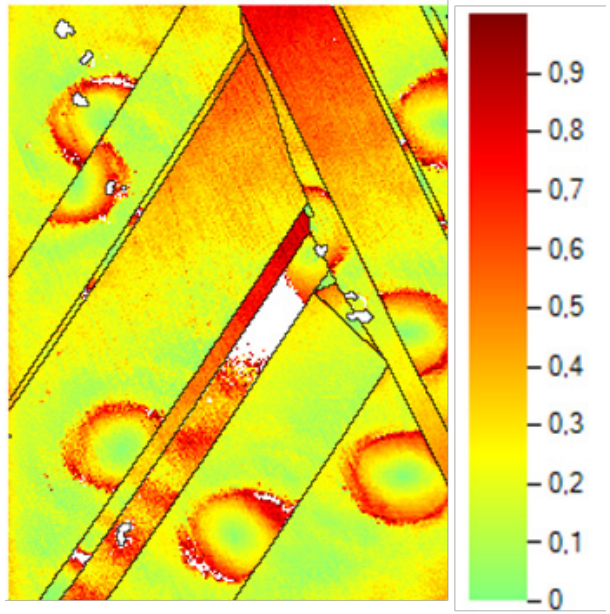

Von Mises stress (GPa)
from cross-correlation

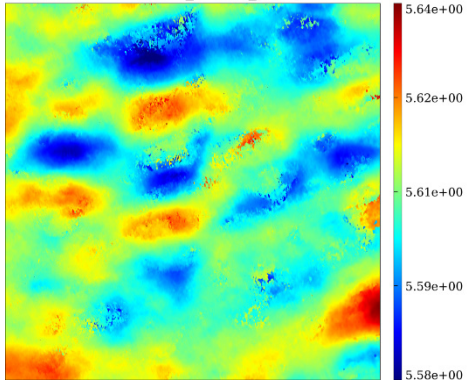

250 µm

250 µm

- **Results (RCI + In situ + Cross correlation) are all consistent.**
- **Additional information**: interaction with the twin boundaries.

Mechanism proposed

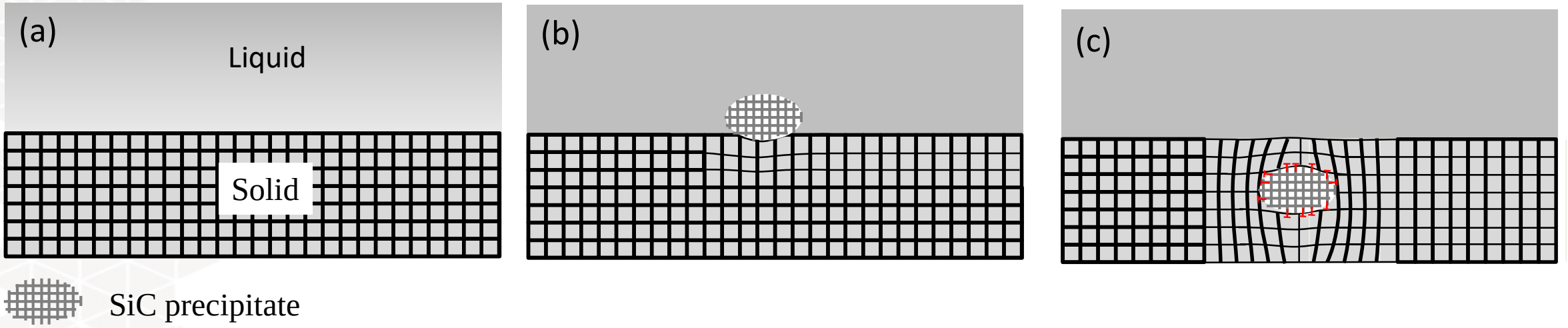

- **SiC precipitates** close to the interface.
- At the level of precipitates **interface is slightly in advance** ⇒ Disorientation between the crystal coming from the **seed** and the one **close to the precipitate** ⇒ **sub-grain formation**

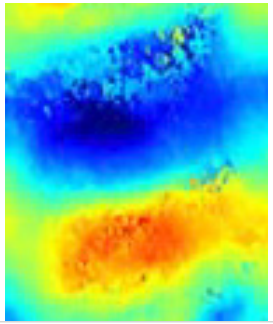

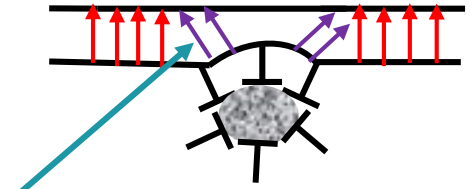

Conclusion

- Combining techniques provide complementary information:
  - **In situ** for **dynamics** and **large scale** (scale of the samples)
  - ESBD for **grain boundary fine characterisation**.
  - RCI for **quantitative measurements of deformation** at **large scale**.
  - Cross-correlation for **deformation and stress determination**.

- Collaboration between IM2NP, MSMP and ESRF:
  - Constant exchanges and cross-feeding.
  - Better understanding of the mechanisms.

Prospects – Ongoing work

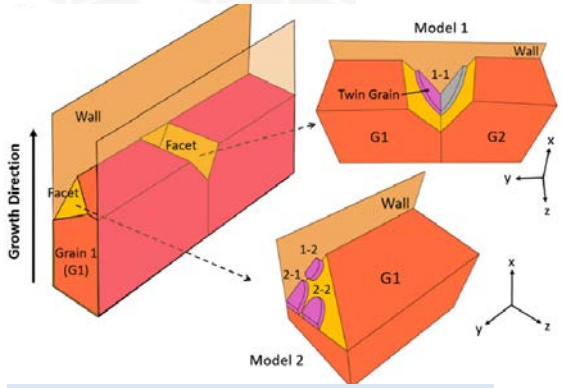

Comparison with numerical simulation
(IM2NP – NTU Taiwan)

J. W. Jhang et al.,
J. Crystal Growth. 508 (2019) 42

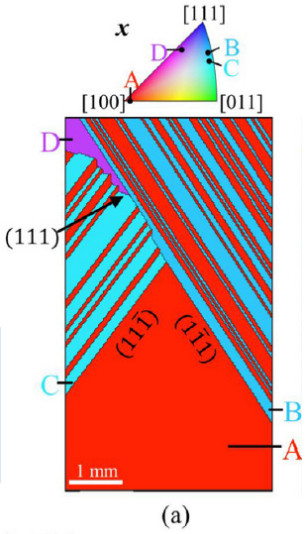

A. Pineau et al.,
Acta Materialia 191 (2020) 1

Comparison with CAFE numerical simulation
(IM2NP – CEMEF-France)

A. Boukhelal et al.,
J. Crystal Growth 522 (2019) 37

3D phase field
(IM2NP)

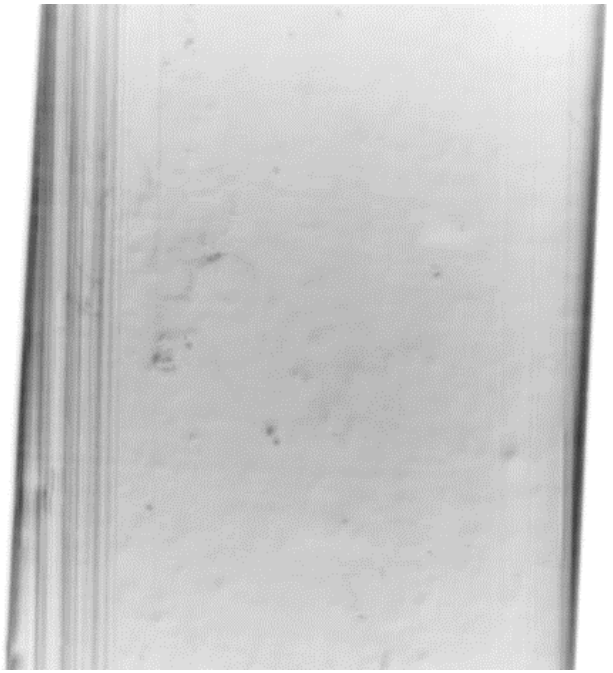

In situ X-ray imaging: Grains, Twinning, Disloctions, Sub Grains
(IM2NP-ESRF)

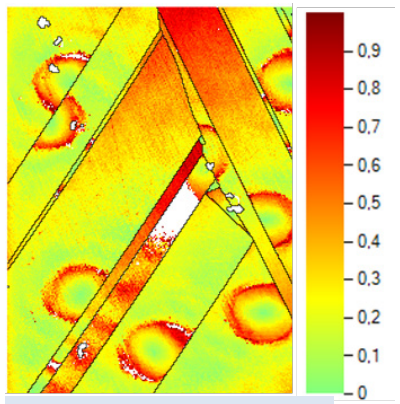

C contamination
(IM2NP-MSMP-ESRF)

M. Becker et al.,
Solar Energy Materials and Solar Cells 218 (2020) 110817

Sub-grain boundaries
(IM2NP-MSMP-INES)

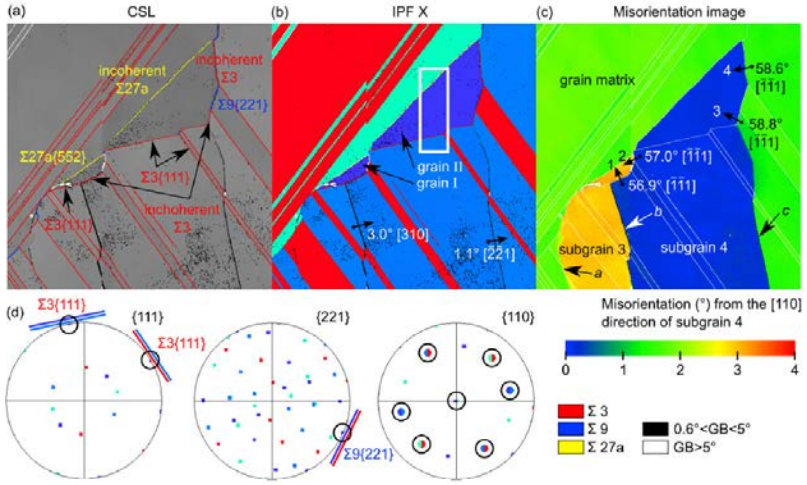

Institut Matériaux Microélectronique Nanosciences de Provence

Merci pour votre attention

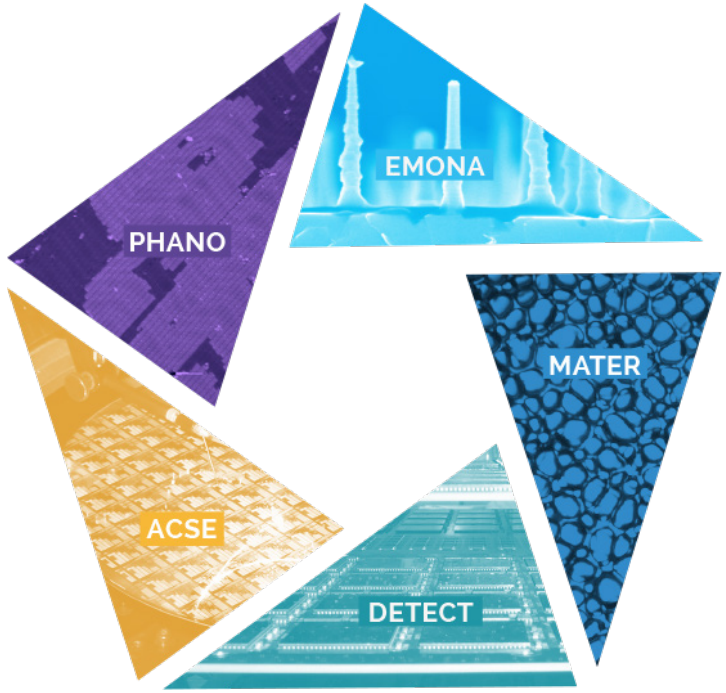

Relier le fondamental aux applications dans nos domaines d'expertise

www.im2np.fr